ELSEVIER

European Journal of Cardio-thoracic Surgery xxx (2007) xxx–xxx

EUROPEAN JOURNAL OF CARDIO-THORACIC SURGERY

www.elsevier.com/locate/ejcts

Review

Regional localisation of left ventricular sheet structure: integration with current models of cardiac fibre, sheet and band structure☆

Stephen H. Gilbert *, Alan P. Benson, Pan Li, Arun V. Holden

Computational Biology Laboratory, Institute of Membrane and Systems Biology & Cardiovascular Research Institute, Worsley Building, Faculty of Biological Sciences, University of Leeds, Leeds LS2 9JT, UK

Received 22 January 2007; received in revised form 12 March 2007; accepted 13 March 2007

Summary

The architecture of the heart remains controversial despite extensive effort and recent advances in imaging techniques. Several opposing and non-mutually compatible models have been proposed to explain cardiac structure, and these models, although limited, have advanced the study and understanding of heart structure, function and development. We describe key areas of similarity and difference, highlight areas of contention and point to the important limitations of these models. Recent research in animal models on the nature, geometry and interaction of cardiac sheet structure allows unification of some seemingly conflicting features of the structural models. Intriguingly, evidence points to significant inter-individual structural variability (within constrained limits) in the canine, leading to the concept of a continuum (or distribution) of cardiac structures. This variability in heart structure partly explains the ongoing debate on myocardial architecture. These developments are used to construct an integrated description of cardiac structure unifying features of fibre, sheet and band architecture that provides a basis for (i) explaining cardiac electromechanics, (ii) computational simulations of cardiac physiology and (iii) designing interventions.

Keywords: Ventricle; Sheet structure; Laminar myocardium; Continuum; Syncytial mesh; Helical ventricular myocardial band

1. Introduction

A heated debate is ongoing in the *Journal* and the wider literature on the morphology of the ventricular myocardium. The current controversy stems from longstanding disagreements — a complete and consistent anatomical description of cardiac structure has proved to be difficult. The heart is a contradiction between the symmetry of helically coursing fibres and regularly stacked laminae with the asymmetry of anisotropic fibre branching and merging of laminae. This complexity has led to the proposition of several incompatible structural models.

One current controversy concerns Torrent-Guasp's concept of the helical ventricular myocardial band (HVMB) — a structural and functional hypothesis that the ventricles are a single band of muscle, coiled into two helices with insertions on the pulmonary trunk and aorta. This model has gained some favour in the medical community, particularly among cardiac surgeons. Indeed, the HVMB has influenced surgical procedures, surgical research and the understanding of the dynamics of heart contraction. However, the HVMB concept has received vigorous criticism of the objectivity and repeatability of the dissection method, its philosophical basis and the failure by its proponents to find or adequately look for independent corroborating evidence. At least eight reviews, one original paper and five letters supporting the HVMB, and six reviews, two original papers and seven letters opposing the HVMB have been published since January 2003. Until recently the argument has been polarised, but Criscione et al. [1] have widened the discussion to a more complex and subtle view of cardiac structure: that there may be regional specialisations of the myolaminar architecture within a continuum meshwork, and that the HVMB may or may not represent a simplification of these regions.

A second area of controversy is on the nature, orientation and degree of anisotropy of the laminar structure of the heart. A non-partisan consideration of both these controversies is presented here. New imaging evidence integrates some features from the opposing models. Based on published evidence, along with our revisualisation of data from diffusion tensor magnetic resonance imaging (DT-MRI), a unifying concept of cardiac structure is proposed which is based on the groundbreaking work of Grant [2].

Excellent historical reviews of heart structural research have been compiled [3,4] and are not recapitulated here.

☆ This work was supported by the European Union through the Network of Excellence BioSim, Contract No. LSHB-CT-2004-005137. S.H.G. is supported by a Medical Research Council UK studentship, A.P.B. by the Dr. Hadwen Trust and P.L. by the Overseas Research Students Award Scheme.

* Corresponding author. Tel.: +44 113 343 4251.
E-mail address: stephen@cbiol.leeds.ac.uk (S.H. Gilbert).

1010-7940/$ — see front matter
doi:10.1016/j.ejcts.2007.03.032

DOCTOPIC: 17, 18, 24

Please cite this article in press as: Gilbert SH, et al., Regional localisation of left ventricular sheet structure: integration with current models of cardiac fibre, sheet and band structure, Eur J Cardio-thorac Surg (2007), doi:10.1016/j.ejcts.2007.03.032

2. Fundamentals of cardiac structure

Along with controversy on macroscopic heart structure there is some disagreement and confusion on microstructural histology and the terminology used to describe this. This is chiefly a result of attempts to fit a simple classification scheme derived from skeletal muscle morphology to the more complicated structure of the heart. We first review and define the terminology.

2.1. Myocytes

Ventricular muscle cells (myocytes) are long, thin cells; their precise dimensions are variable depending on species, age and cardiac location, but are within the approximate range of 50–150 μm in length and 10–20 μm in diameter [3,5–8]. They are joined to their neighbours via intercalated discs at their ends. Terminal abutments are usually with more than one cell [3,9]. Being long extended cells, myocytes possess a principal direction given by the long axis of the cell, and the ellipsoidal myocardial nuclei are aligned to this axis [10–13].

2.2. Myofibres and myolaminae

In skeletal muscle morphology, myofibre has an absolute definition. In cardiac morphology it has different meanings to different researchers. Streeter [3] uses the term as a synonym for the myocytes. Other groups [4] use the term to indicate groups of three or more myocytes surrounded by a perimysial weave. The term myolaminae has been introduced [9] to describe sheet-like cleavage planes of attached myocytes (Fig. 1d–g). Some controversy exists regarding the form of laminae within the living heart. Some researchers [4,8,14], although recognising the existence of laminae, have played down their significance, emphasising instead the mesh-like nature of cardiac structure. The evidence presented in this review points to myolaminae and the groups of myocytes surrounded by a perimysial weave being a continuum of structure; therefore, we use myofibre to refer to individual myocytes and myolaminae to refer to these groups of myocytes. The term fibre is used by some groups to denote a continuous axial sequence of individual myocytes [15]. We use this term to denote the net axial direction of myocytes at a specific cardiac location, always with consideration of the important caveats in defining such a continuous axial sequence (as discussed in Sections 4 and 6). Likewise, the term *sheet* is related to the myolaminae but has a looser definition – describing the planar features of the myocardial wall, both the myolaminae and the cleavage planes between myolaminae [16].

2.3. Interlinking and merging of cardiac microstructure

Simplified connective tissue structure diagrams are often presented in reports of cardiac microstructure, but they can be misleading as they suggest a rigidity of structure. The key feature of cardiac microstructure is the interlinking and merging of structural elements; fibres link with several others at their poles, myolaminae coalesce and divide (visible in careful inspection of Fig. 1e) and fibres run from one myolaminae to another, all surrounded and supported by

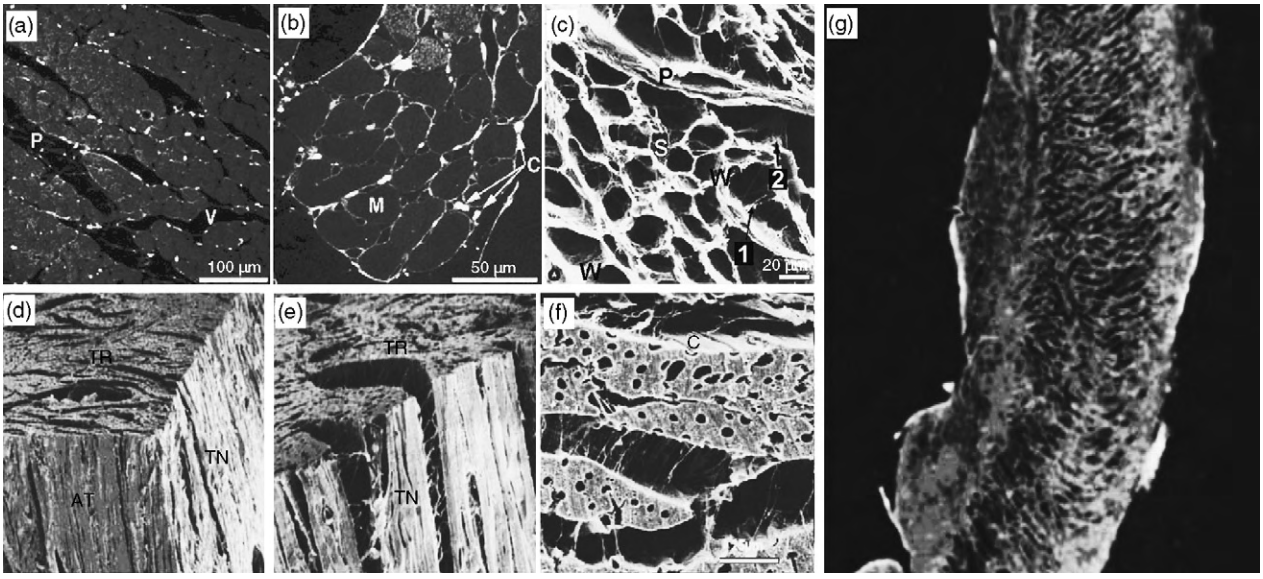

Fig. 1. Microscopic cellular and intercellular (a–f) and macroscopic (g) tissue structure of the LV wall. (a) Lower magnification and (b) higher magnification optical images of a rat LV midwall stained with picrosirius red. Endomysial collagen surrounding individual myocytes is evident. M, myocytes; C, collagen cords; V, vascular structures; P, cleavage planes. (c) Honeycomb connective tissue skeleton revealed by scanning electron microscopy of human heart. The perimysium (P) envelops groups of myocytes. The endomysium, as final arborisation of the perimysium, supports and connects individual cells. The endomysial weave (W) envelops each individual myocyte and is connected to adjacent myocytes by lateral struts (S) presenting branches of variable size and extension. The range of length and diameter of these struts is very wide. Collagen struts also connect myocytes to interstitial microvessels (arrow 1) or perimysium (arrow 2). (d–f) Scanning electron micrographs showing three orthogonal surfaces of a typical left ventricular midanterior midwall specimen: (d) oblique view of tangential (TN), axial transmural (AT) and transverse (TR) faces of specimen; (e) view of TN and TR surfaces; (f) TR surface. Perimysial connective tissue weave surrounding myocardial sheets is evident and covers surface capillaries (C). (g) Micrograph of longitudinal–transmural section of left ventricle showing the radial alignment of myolaminae [(a and b) from Young et al. [20] with kind permission from Blackwell Publishing; (c) from Rossi et al. [93] used with permission; (d–g) from LeGrice et al. [56] used with permission].

Please cite this article in press as: Gilbert SH, et al., Regional localisation of left ventricular sheet structure: integration with current models of cardiac fibre, sheet and band structure, Eur J Cardio-thorac Surg (2007), doi:10.1016/j.ejcts.2007.03.032

a complex collagen and elastin network. As with fibre nomenclature, connective tissue terminology is derived from skeletal muscle morphology. In its application, attention must be paid to the multi-level complexity of ventricular microstructure.

2.4. Endomysium

Each myocyte is wrapped in a prominent sheath of endomysium which supports the Z-bands and basal laminae [17]. The endomysium is seen in picrosirius red-stained confocal images (Fig. 1b), high-power scanning electron micrographs (not shown) and sodium hydroxide digestions (Fig. 1c).

2.5. Perimysium

The perimysium unites the myolaminae as units, from within, via collagen struts linking adjacent myocytes (120–150 nm) (Fig. 1b), and exteriorly as a weave of connective tissue (Fig. 1c and f). Long perimysial collagenous tendons link connective tissue of adjacent myolaminae (Fig. 1a, b, e and f).

2.6. Epimysium

This term is of little value in cardiac morphology. In skeletal muscle it represents the outer smooth collagen layer of the muscle belly which makes no fibrous connections from its external surface – the cardiac equivalent is only present at endocardial and epicardial surfaces.

3. Models of heart structure

Seven conceptual models of cardiac structure are summarised in Fig. 2. The variety of proposed structures is visually striking – this is due, in a large part, to the different levels of cardiac structure described (discussed in detail in Section 4). Model 6 (Fig. 2, part 6) groups the myocardium into regional functional units analogous to skeletal muscles. Models 1–5 (Fig. 2, parts 1–5) are continuum concepts – stressing to differing degrees the anisotropic interconnectivity inherent in cardiac structure. Models 1 and 2 (Fig. 2, parts 1 and 2) describe fibre orientation. Model 3 (Fig. 2, part 3) describes changes through layers from epicardium to endocardium. Models 4 and 5 (Fig. 2, parts 4 and 5) examine the myolaminar structure, with less emphasis on fibre orientation. Some descriptions of Model 7 (Fig. 2, part 7), the HVMB, have emphasised discrete structural bundles [18] while other reports have proposed the band within a continuum framework [8].

4. Philosophical approach for description of a complex structure

How can so many models co-exist? Some must be wrong – or is it possible that different models are true representations of the heart when considered from different perspectives? One 1965 review on cardiac structure stands out as a philosophical foundation upon which all future studies should be based. Robert P. Grant, M.D., in his *Notes on the Muscular Architecture of the Left Ventricle* [2], puts forward the following principles (along with an excellent description of cardiac structure):

(1) as evidenced from numerous dissections, a given fibre segment has branching connections with other fibre segments in several different directions – as such the myocardial structure is a syncytium-like arrangement [19],
(2) the cardiac structure problem is therefore a three-dimensional network problem,
(3) structure understood from study of the network depends on the level on which the structure is approached; whether an attempt is made to describe the predominant behaviour in the entire ventricle(s) or at the other extreme, to describe the average branching from a specific location,
(4) many models of heart structure can therefore be proposed depending on the conceptual approach,
(5) statistical study of the branching must be added to geometry for an accurate picture of myocardial architecture,
(6) in consideration of such statistical problems one approach is to construct models for different degrees of generalisation of the problem,
(7) no single model gives the whole story but together they provide a schema,
(8) the existence of a syncytium-like arrangement does not in itself dictate that no separate 'bundles' are present; however, due to the complex structure it is possible to construct by dissection bizarre arrangements which have no underlying anatomical reality,
(9) any dissection of the myocardium may represent (a) a valid schema from an infinite set of valid schema, (b) a bizarre and meaningless pathway or (c) a grouping of fibre paths within the syncytium of such general shared fibre direction that it can be considered a physiological or anatomical *bundle*,
(10) a unique anatomical bundle is not the same as a unique physiological bundle – a connection between separate anatomical structures may produce one physiological structure,
(11) a statistical approach is required to demonstrate any independent anatomical entity.

When viewed from this perspective it is not surprising that many models exist, that these are not all mutually compatible and that argument continues. Further evidence for these principles is presented in a dissection study by Fox and Hutchins [19], where principle (1) is re-stated and emphasised: '*The only level of the network of cells that can be referred to accurately as a fibre is a single cell. The 'fibre' is often only one cell in length before it splits and branches*'.

When considering the structural debate it is logical to return to Grant's principles – an approach adopted in this review. It should be noted that although Grant suspected regional variations in fibre branching within the left ventricle, he was sceptical whether these local prevalences would statistically warrant consideration as separate

Please cite this article in press as: Gilbert SH, et al., Regional localisation of left ventricular sheet structure: integration with current models of cardiac fibre, sheet and band structure, Eur J Cardio-thorac Surg (2007), doi:10.1016/j.ejcts.2007.03.032

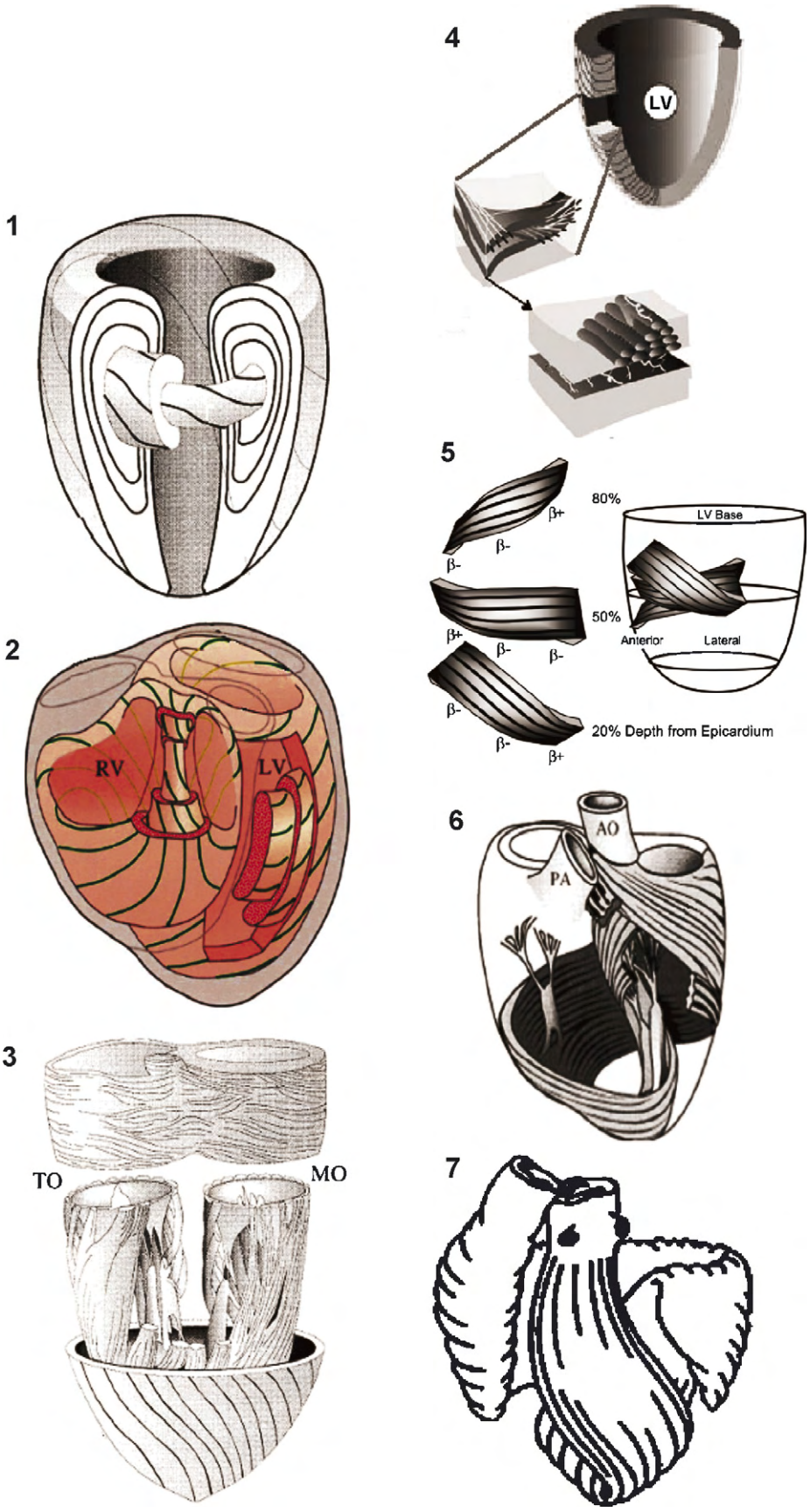

Please cite this article in press as: Gilbert SH, et al., Regional localisation of left ventricular sheet structure: integration with current models of cardiac fibre, sheet and band structure, Eur J Cardio-thorac Surg (2007), doi:10.1016/j.ejcts.2007.03.032

bundles. One feature of the myocardial structure problem Grant did not consider was that significant structural differences may exist between individuals of the same species – a question discussed at length later in this review.

5. Traditional and novel techniques

Traditional anatomical techniques have several limitations which have made it difficult to apply Grant's principles: (i) dissections and histological studies are subjective; (ii) the techniques are better suited to qualitative rather than quantitative descriptions, so the application of statistical analysis is difficult; (iii) the techniques are destructive and (iv) the reconstruction of three-dimensional fibre and sheet orientation from two-dimensional sections has been difficult [3].

Recent technical developments have greatly contributed to the available data on cardiac structure. Automated confocal microscopy methods have allowed extended imaging of three-dimensional tissue at high resolution, clearly demonstrating laminar structure [20,21]. Optical methods, including polarisation microscopy, have allowed demonstration of fibre orientation in the whole heart [22,23].

Whole heart fibre and laminar structure have been revealed by DT-MRI, a three-dimensional technique which uses MRI to provide the axes of diffusion of protons of water molecules in tissue. Detail of tissue architecture is imaged by its restriction of the random movement of the protons. The pattern of diffusion is represented mathematically by a symmetric second-rank tensor in three-dimensional space, which can be written as a 3×3 matrix. The three orthogonal eigenvectors of this tensor (ranked in order of their magnitudes of their corresponding eigenvalues) have been related to cardiac structure, with the eigenvalues representing the diffusion along three principal axes. Theory suggests that the direction of greatest proton diffusion (i.e. the eigenvector with the largest eigenvalue, the primary eigenvector) will be along the fibre long axis, intermediate diffusion (the secondary eigenvector) will lie in the myolaminae plane, orthogonal to the fibre long axis. The third and minor direction of diffusion (the tertiary eigenvector) is by definition orthogonal to the primary and secondary eigenvectors, so is normal to the myolaminar plane. The correspondence between the primary eigenvector and fibre orientation, and the secondary and tertiary eigenvectors and sheet orientation has been validated by combined DT-MRI and three-dimensional histological reconstruction of fibre and sheet structure [9,13,24–27].

An advantage of whole heart DT-MRI and optical methods is that they can provide digital datasets that can be analysed and compared algorithmically at high speed. They are, therefore, inherently suitable for statistical analysis. The bias, resolution and selectivity for the architectural characteristic measured apply equally across the entire heart. Examination of data from these techniques is therefore highly suited to identification of grouped fibre paths, which satisfy Grant's criteria for uniqueness; the validity of structural models is discussed in this light.

6. Doughnut and pretzel models — Models 1 and 2 (Fig. 2, parts 1 and 2)

The fibre path models are based on the synthesis of many measurements of angles of fibre orientation through the ventricular wall and differ primarily in their scope (Model 1 is left ventricle (LV) only; Model 2 is LV and right ventricle (RV)). No argument is made for discrete traceable fibre paths – rather a recognisable general fibre trajectory [3]. These models reconstruct the long accepted helical pattern of fibre orientation, which has recently been confirmed by DT-MRI [30,35–40] (Fig. 3). DT-MRI fibre-tracing algorithms (Zhukov and Barr [28] and Kondratieva et al. [29], applied to canine data; Schmid et al. [30], applied to porcine data; Rohmer et al. [31], applied to human data) and automatic computational constructive visualisation methods (Chen et al. [32,33] and Fig. 15(B) in [8]), used to extract meaningful visual information from histologically recorded three-dimensional fibre orientation datasets [33,34] (recorded from the rabbit heart), produce models remarkably similar to that proposed by Streeter (Fig. 2, part 1).

Fig. 2. Models of mammalian ventricular architecture. (1) LV as nested doughnut (toroidal) geodesics (synthesised by Streeter [3] from work of Krehl [49], Hort [54] and reconstructed by Jouk et al. [23] (see Model 2)): assumes myocardium is a specialised form of vascular musculature, with myocardial fibres as a network of preferentially orientated and branched myocardial cells forming end-to-end cellular junctions. The fibres follow paths of shortest length (geodesics) nested on doughnut-shaped surfaces (toroidal bodies of revolution). (2) LV and RV as nested pretzel geodesics (Jouk et al. [23]): extension of Model 1 to describe both left and right ventricles, based on data from quantitative optical polarisation microscopy of the foetal human heart. Fibres follow geodesic trajectories on nested warped pretzels, where a pretzel is two side-to-side joined doughnuts. (3) Three-layered ventricle (proposed by Rushmer et al. [48] and developed by Anderson et al. [4] and others): the ventricles are composed of superficial, middle and deep layers. The fibres follow a continuum or functional syncytial mesh (FSM) with multiple branching and cannot be split down further into functional units. There is a net helical fibre orientation across and within the ventricular walls [4]. Some debate has occurred between proponents of this view regarding the degree of fibre penetration between layers. (4) Simple laminar structure (proposed by LeGrice et al. [56]): the myocardial wall consists of an ordered laminar structure, separated by extensive cleavage planes that run approximately radially from endocardium to epicardium. In tangential sections the plane of the laminae coincides with local fibre orientation. Layers are about 4 ± 2 myocytes across and 48.4 ± 20.4 μm thick (in the dog). Components of the connective tissue matrix connect adjacent laminae. (5) Complex laminar structure: strain modelling, histological and DT-MRI studies [9,11,13,44,45,58] have revealed evidence of two approximately normal myolaminae populations. More complex features of cardiac structure have been described to account for this evidence, but have not been formalised or organised into complete conceptual structural models. However, one early model has been proposed by Harrington et al. [11] and is shown here. (6) Distinct muscle bundles (DMB): Robb and Robb [61], following from Mall [94], consider cardiac structure analogous to skeletal muscle – fibres gathered in distinct bundles to form muscle bellies. Four muscle bodies proposed, anchoring to the fibrous trigones and aortic and pulmonary roots. (7) Helical ventricular myocardial band (HVMB) (Torrent-Guasp et al. [8,18,62,95]): both RV and LV exist as a single muscle band: the HVMB, organised spatially as a helix and consisting of basal and apical loops. This band is a helical rope-like structure that is unrolled easily from the heart by blunt dissection along natural cleavage planes – that follow the *principal fibre direction* at any point. A connective tissue sheath enclosing the band segments was not proposed [diagrams for Models 1, 2, 3 and 6, adapted from Jouk et al. [23] with kind permission from Springer Science and Business Media, Model 4 from LeGrice et al. [56] used with permission and Model 5 from Harrington et al. [11] used with permission. Model 7 from Kocica et al. [8] used with permission].

Please cite this article in press as: Gilbert SH, et al., Regional localisation of left ventricular sheet structure: integration with current models of cardiac fibre, sheet and band structure, Eur J Cardio-thorac Surg (2007), doi:10.1016/j.ejcts.2007.03.032

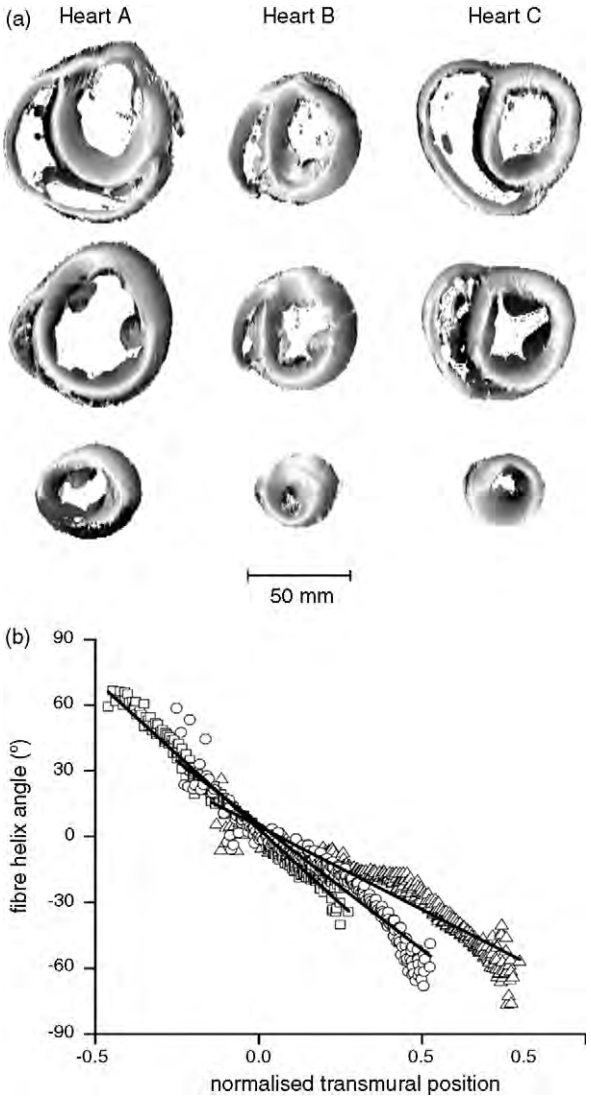

Fig. 3. (a) Smooth changes in DT-MRI derived fibre helix angles in canine heart, short axis basal (top), equatorial (middle) and apical (bottom) slices from three hearts A, B and C. The fibre helix angle is the angle between the transverse plane and the projection of the primary eigenvector onto the tangential plane. The shading shows the absolute value of the angle using a grey scale, such that white indicates fibres lying in the transverse plane and black indicates fibres normal to this plane. (b) Combined transmural fibre helix angle from 15° sectors in the interpapillary muscle region of the equatorial slice of three canine hearts. Data are aligned at the midwall where normalised position = 0.

Peskin [41] has carried out an asymptotic analysis of Model 1 and has derived the fibre architecture of the heart from first principles.

These models form a conceptual model of cardiac structure from the one macro- and microscopically observed characteristic of principal fibre direction. As such, the nested doughnuts/pretzel surfaces are abstract concepts — no discrete biological equivalents exist. It is possible to create the surfaces by dissection following the observed principal fibre direction, as demonstrated in early studies by Torrent-Guasp [3,42], but in so doing much information is lost. The dissection and histological methods used do not record data of local branching in directions other than the predominant fibre orientation, so by definition no detail of local tissue organisation is modelled. Locally branching fibres are *smoothed* to a single orientation, which is again *smoothed* to a global ventricular fibre orientation. With reference to Grant's principles, these models represent the highest order schema of whole heart fibre orientation in isolation.

It might be assumed that the fibre maps produced by algorithmic analysis and computer visualisation may be more than a conceptual model, but the considerations above apply equally. The DT-MRI fibre-tracing algorithms track the principle fibre orientation from the primary eigenvector only. The automatic computational constructive methods were applied to histological fibre orientation datasets which only record principle fibre orientation. Being limited to tracking the principle fibre orientation alone, these methods cannot reconstruct any detail of myolaminar structure, and as such reproduce idealised fibre-tracing dissections.

Much evidence points to myolaminae as the central feature of the wall motion mechanism [16,43–46]. As such the doughnut and pretzel models represent geometric abstractions of cardiac structure. Their primary uses may be in (i) refining more *histologically* detailed models for the constraint of fibre orientation and (ii) in modelling the spread of the cardiac action potential, the conduction of which is significantly influenced by principal fibre direction [47].

7. Three-layered myocardium — functional syncytial mesh — Model 3 (Fig. 2, part 3)

This model is similar to the fibre path models (Models 1 and 2). It divides the myocardium into three layers on the basis of fibre orientation. It was put forward by Rushmer et al. [48] as a mechanistic model of cardiac contraction, in which (as first proposed by Krehl [49]) the middle circular layer acted as a constrictor. Further studies endorsed and extended this description [15,50–52]. Paradoxically, these later studies endorse this model whilst also accepting that the separation of layers is artificial as the orientation of fibres changes gradually, and there are fibres which span layers: '*As a result we can differentiate three layers of fibres: superficial (subepicardial), middle and deep (subendocardial). However, it is very important to emphasize that the separation of these three layers is artificial since the change of the direction of the fibres is gradual without cleavage planes of connective tissue. Moreover, a number of fibres change layers in their trajectory around the ventricles*' [15].

As with the previous models, the features described in the three-layer model are largely correct — this is not surprising given the many anatomical dissections upon which the model is based. However, as described, the model is vague or contradictory in its description of the boundary zones between layers, where evidence points to a smooth transition of principal fibre direction through the myocardium. Laminar structure is omitted in early descriptions of the model and, although now accepted by some proponents [4], its higher-level symmetry and regional patterning remain unappreciated.

Please cite this article in press as: Gilbert SH, et al., Regional localisation of left ventricular sheet structure: integration with current models of cardiac fibre, sheet and band structure, Eur J Cardio-thorac Surg (2007), doi:10.1016/j.ejcts.2007.03.032

8. Simple myolaminae model — Model 4 (Fig. 2, part 4)

Sheet structure was first described in detail by Feneis (cited by Hort in [54]) and then Hort [53–55]. Hort described macroscopic sheet structure visible in dissections as *feathering* or *pinnation*, and understood these areas to be regions of reduced fibre and connective tissue interconnectivity between sheets of myocardial cells. Grant [2] described parallel fibres, which 'by their branching form planes that seem to rotate'. Spotnitz et al. [46] not only described open spaces between planes in rat heart histology but also proposed that sliding between these planes accounted for the change in myocardial volume associated with contraction. Greenbaum et al. [50] referred to the grossly visible structures as *layers* and described them as regions of little change in fibre orientation in contrast to regions of rapid change, but disputed different connective tissue morphology between and within layers.

LeGrice et al. conducted the first quantitative analysis of sheet structure and formalised this into a conceptual [34,56] and mathematical [57] laminar model of cardiac structure in which the canine myocardial wall is organised with an ordered laminar structure, separated by extensive cleavage planes and running radially from endocardium to epicardium, integrating whole heart fibre orientation. Examination of the long-axis cut surface of the LV allows myolaminae to be identified without magnification (Fig. 1g). Viewing this image from a distance allows the identification of radial myocardial sheets, but the eye oversimplifies the structure — close-up inspection reveals a highly branched topology with two approximately perpendicular (strictly normal as in three dimensions) sheet populations.

Although the authors of this model recognised regional anisotropy in sheet structure, they underestimated its degree and significance which was recognised by Feneis (cited by Hort in [54]) and has recently been highlighted in several studies [9,11,13,44,45,58]. A mathematical analysis of the co-existing regular helical fibre path and LeGrice's proposed sheet structure (in the manner of Peskin [41] for fibre path alone) has not been carried out, but these features do not seem compatible.

9. The helical ventricular myocardial band — Model 7 (Fig. 2, part 7)

This is a structural and functional hypothesis that the ventricles are a single band of muscle, coiled into two helices with insertions on the pulmonary trunk and aorta. The concept is based on Torrent-Guasp's dissection method, where the predominant fibre direction at given point is followed in hearts boiled in 1% ethanoic acid. Aberrant fibres, going against the plane of dissection, are recognised but are torn in the process of the dissection.

9.1. HVMB topology

The concept of the ventricular myocardial band is very simple: there are two loops each divided into two segments (basal loop — right and left segments; apical loop — ascending and descending segments). The connectivity and anatomical arrangement of these four segments is shown in Fig. 4a.

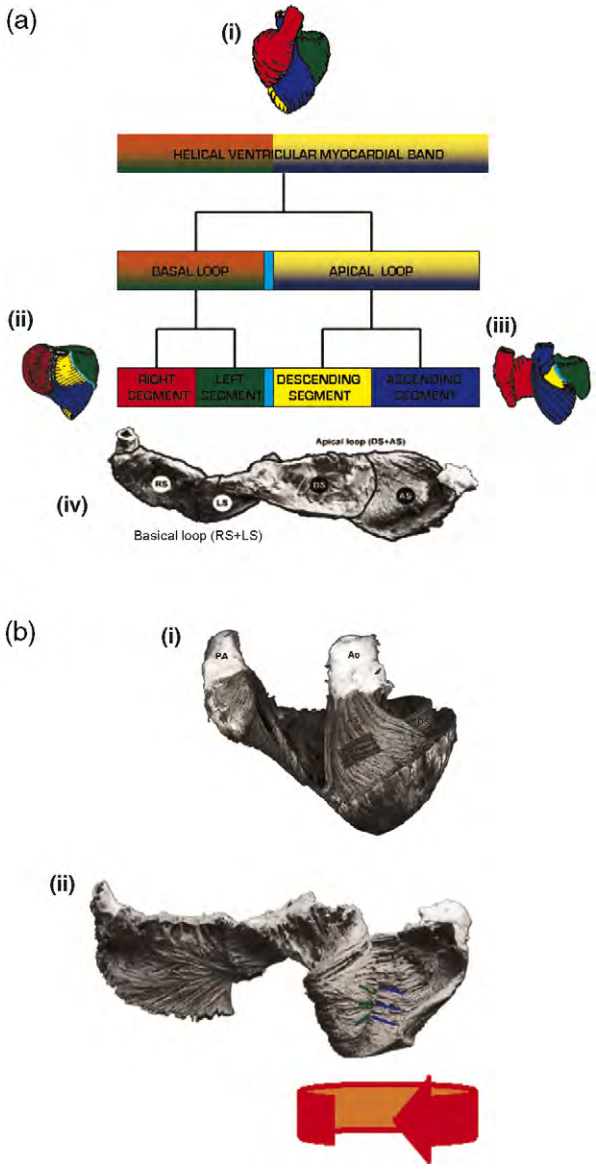

Fig. 4. (a) The topology of the HVMB. The dendrogram illustrates the band hierarchy with the same colour scheme used in the images: (i) band segments colour-coded on the intact heart; (ii) RV cut away to reveal deeper fibres; (iii) start of HVMB dissection — separation of the RS from the AS, and rotation around the aortic root; (iv) the unrolled myocardial band [modified from Kocica et al. [8] (a video of the dissection can be viewed at http://www.helicalheart.com/video_right.htm)]. (b) A partially reconstructed image of the ventricles from the HVMB dissection. The red arrow indicates how the dissection planes are re-apposed, and the green and blue lines show the surface fibre orientation. The angle of fibre orientation is approximately the same on either side of the dissection plane. The choice of this dissection path was therefore on minimal difference: (i) a block is cut out of the HVMB ascending segment of a near fully reconstructed heart. Through the cut out surface fibres of the descending segment can be seen and are orthogonal to the visible surface fibres of the ascending segment. What is not shown is that the fibre angle changes continuously throughout the cut out slab such that fibre orientation in the ascending segment and descending segment are almost identical on the plane where they meet as observed in (ii) [adapted from Kocica et al. [8], used with permission].

Please cite this article in press as: Gilbert SH, et al., Regional localisation of left ventricular sheet structure: integration with current models of cardiac fibre, sheet and band structure, Eur J Cardio-thorac Surg (2007), doi:10.1016/j.ejcts.2007.03.032

9.2. Presentational problems

Early reports of the HVMB describe a '*unique morphologic and physiologic characteristic*' of '*unique anatomy*' that '*unwrap[s] along a natural cleavage plan*' [18]. Although an enclosing connective tissue sheath is not proposed, the band could be considered a muscle belly in all except epimysium. Indeed some [59], after reading this description, have understood Torrent-Guasp to be describing connective tissue sheaths between band segments. A recent description [8] has highlighted the '*infinite anisotropy of the ventricular myocardium*', recognised a '*functional syncytial mesh, resembling vascular musculature*' and also that '*blunt anatomical dissections following predominant fibre direction, shall reveal unique functional (i.e. vectorial) but not any eclectic (i.e. discrete) anatomical planes in the ventricular mass*'.

The continuum concept has always been present in the HVMB literature; in earlier descriptions it was underplayed [18,42,60] but has recently received greater emphasis [8]. While it cannot be expected that an idea will remain static over 30 years, the evolution of the concept is not clearly set out and this has increased confusion in the HVMB debate. This confusion is compounded by the presentation of images and diagrams of the HVMB dissection which create a false impression of the band's discreteness (Fig. 4b). Images of the same dissections in different orientations would emphasise the continuum of structure across band segments.

9.3. Philosophical problems

The HVMB has been dismissed on the basis of histological, optical [23] and DT-MRI [30] evidence of the smooth change in ventricular fibre orientation across the myocardium, as described in the geodesic models and shown in Fig. 3. If fibre angle changes smoothly across the wall with no glitches, how can the band exist? This argument against the band appears powerful, but is flawed. Grant's principles allow for the presence of discrete localisations of branching within a smoothly changing whole ventricle predominant fibre orientation schema. Recent evidence has been found for regionally anisotropic distribution of two sheet populations (discussed at length in Section 10.2). Could this regional sheet anisotropy represent the HVMB?

A more complete consideration of the HVMB requires separate analysis of (i) the merits of the dissection, (ii) the static structural model and (iii) the dynamic concept formulated on the basis of the structure.

A first consideration is that, by Grant's principles, any dissection path followed in the ventricles is a statistical concept. An implication is that if a path is sought from any point to any other within the ventricles it can by definition be found. In fact, infinite paths can be found, and again by definition, one path will also be most statistically favoured. Being the most favoured path alone does not necessarily make the path sensible or informative.

Is the HVMB (i) a bizarre and meaningless pathway, (ii) one of an infinite set of valid schema, (iii) a useful schema of structural features at one level of abstraction of cardiac structure or (iv) a grouping of fibre paths within the syncytium of such general shared fibre direction that it can be considered a unique physiological or anatomical entity (as proposed by Torrent-Guasp et al.)? The answer depends on both the statistical analysis of the fibre branching along the dissection path and on a detailed study of the macro- and microstructural boundary zone between HVMB segments. If the band is one dissection out of infinite possible dissections, each dissection will have a statistically derivable value calculated from the predominance of fibres following the chosen path at each point along its length. The validity of the band can be judged from the significance of the difference between the HVMB and other possible dissections (i.e. the *p*-value).

As discussed above, the HVMB has been rejected by some on the basis of histological [4,14], optical [23] and DT-MRI [30] evidence of the smooth change in ventricular fibre orientation across the myocardium (Fig. 3) There is, however, convincing and conflicting evidence that the HVMB *does* follow a favoured path from histological [54], optical [22] and DT-MRI data presented in Fig. 5. This figure synthesises fibre angle change, obtained from DT-MRI, with the dissection diagrams of Hort [54] and optical section reconstructions of McLean and Prothero [22]. Both longitudinal DT-MRI (fibre angle change) sections and the optical reconstruction split the ventricles into zones clearly reflecting the HVMB dissection planes.

DT-MRI-derived cross-sections show V-shaped features correlating to the pinnation features described by Hort [54]. If a dissection plane is made joining these features this reproduces a key feature of the HVMB dissection path. Streeter [3] described the linking of the V-shaped pinnation features in this manner to produce the discrete muscle bundles described by Robb and Robb [61] (Model 6). This evidence does not identify the HVMB as a unique unit but it does show that the dissection of Torrent-Guasp et al. follows, at least in part, a measurable difference within the myocardium. Visualisation of canine myocardial sheet angle (Fig. 8c and d; discussed in detail in Section 10.3) provides yet more convincing evidence that the HVMB follows real anatomical features.

This evidence of a favoured dissection path is *not* a justification of the HVMB structural model. Examination of high-resolution three-dimensional microscopic images show that (in rat heart at least) the band dissection plane tears across structural features of a complex continuum of merging sheet populations running from epicardium to endocardium (Fig. 6a–c; discussed in detail in Section 11). Laminar sliding and extension have been demonstrated as the most significant component of systolic ventricular thickening [44], and although strain modelling studies are only beginning to extend to consideration of two sheet populations [44,45,58], evidence points to interactions between sheet populations (in three dimensions) being key to LV radial wall thickening in systole.

The HVMB dynamic concept proposes independent band action via longitudinal sliding of HVMB band segments [62,63], and studies have revealed some division of dynamical properties across band regions [63,64]. This is not unexpected as different band areas have differing fibre and laminar structure. This evidence should not be interpreted as justification of the HVMB structural–functional concept, as it is incompatible with microstructural evidence.

Please cite this article in press as: Gilbert SH, et al., Regional localisation of left ventricular sheet structure: integration with current models of cardiac fibre, sheet and band structure, Eur J Cardio-thorac Surg (2007), doi:10.1016/j.ejcts.2007.03.032

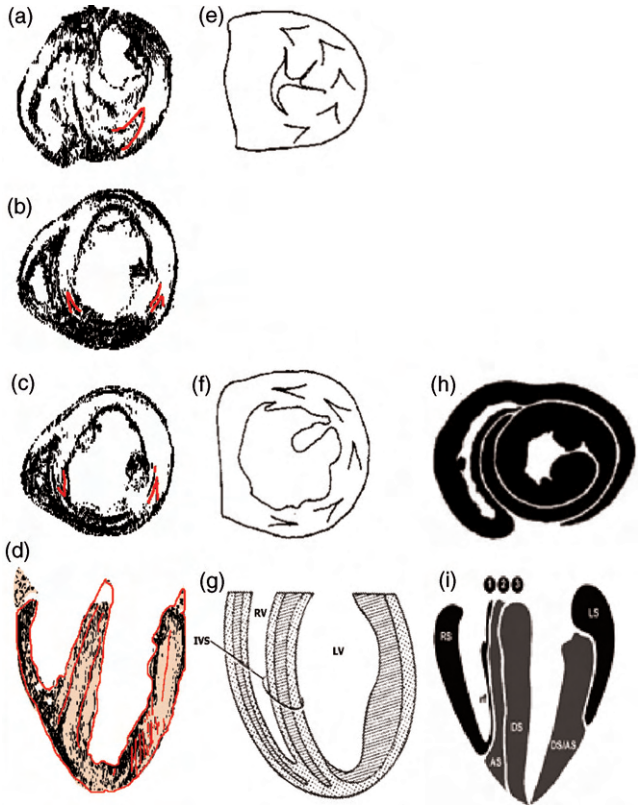

Fig. 5. Synthesis of maps of fibre orientation obtained from DT-MRI with ventricular architecture from histology. (a–d) Radial transitions in canine DT-MRI primary eigenvector (fibre orientation). Divergences above 6° are shown in black in (a) basal heart B (fixed approximately in systole); (b) basal heart A (fixed approximately in diastole); (c) mid-heart heart A; (d) anterior long-axis view heart C (fixed approximately in diastole). Major transitions highlighted in red. (e, f) Canine histological pinnation patterns observed by Hort in (e) systole and (f) diastole. The angle formed by the pinnation (between the arms which form the V shape) is greater in systole (a, e) than in diastole (b, c, f). (g) Longitudinal reconstruction of murine optical mapped fibre angle by McLean and Prothero [22]; and (h, i) diagrams of cross-sections of the HVMB dissection [(a–d) novel analysis of DT-MRI data by the authors; (e, f) adapted from Hort [54] with kind permission from Springer Science and Business Media; (g) adapted from McLean and Prothero [22], used with permission; (h) from Torrent-Guasp et al. [60], used with permission; (i) from Kocica et al. [8], used with permission]. All transverse sections viewed from above, all longitudinal sections viewed from anterior position.

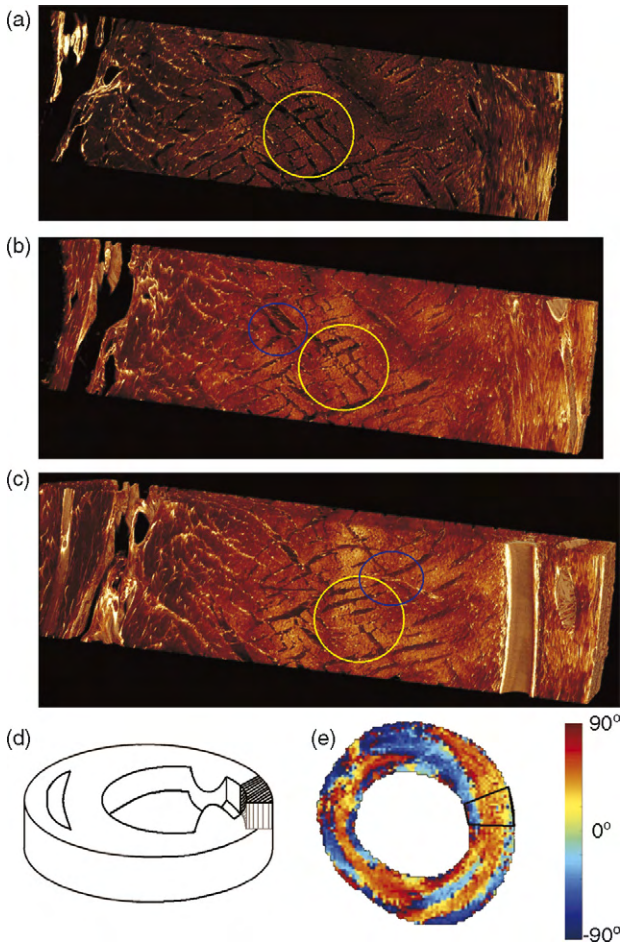

Fig. 6. (a–c) Two co-existing sheet populations in the serially confocal imaged rat ventricle. Images used with permission from dataset described in Sands et al. [21] and reconstructed from the video which can be viewed at http://www.bioeng.auckland.ac.nz/movies/database/cardiovascular_system/B24b_scan.avi. The outermost face of the tissue block is the longitudinal–radial cardiac plane. As the video runs from (a) through to (c) additional longitudinal–radial layers are added, such that the transverse cardiac plane (to the top of the block) becomes increasingly visible as a surface. As video runs from (a) through to (c) the co-existence of ~+45° and ~−45° sheet orientations (β'-sheet angle), and the merging of these into central longitudinal myolaminae (of roughly rhomboid cross-section – highlighted in the yellow circle) can be seen. The two sheet populations can be observed to co-exist in the regions identified by blue circles. The looseness (spacing) of the laminae in the merge region is evident. (d) Identifies the cardiac location of the interpapillary mid-heart tissue block which was serially confocally imaged (modified from [20]). (e) Rat cardiac βs-sheet angle reconstructed from DT-MRI [from Chen et al. [16], used with permission]. The +90° → −90° colour scale bar is shown. The highlighted region of this transverse slice corresponds to the transverse surface shown in (d). The DT-MRI imaged region is therefore representative of a transverse slice of the confocal imaged tissue block in (a–c). The sheet angle reported here is βs, and was set as positive for a sheet orientated towards the base from endocardium to epicardium. The global sheet features seen in the confocal imaged tissue block are also seen in the DT-MRI determined βs-sheet angle.

At best, the HVMB dissection represents one generation of Grant's schema of cardiac structure, but as described above, it misleads more than it informs. More useful schema are in the form of the DT-MRI transition data, which demonstrate boundaries of subtly different fibre orientation without overemphasising their importance by tearing and then refolding them as distinct units.

10. Unifying structural model

10.1. Terminology for local aggregations of structure

Primary cardiac structure has been defined as the predominant fibre orientation, secondary as the organisation of the myolaminae through which these fibres course, and tertiary structure as localised aggregations of primary and secondary structure (often referred to as bands) [4,14,65,66].

Some cardiac researchers have dismissed the presence of localised aggregations of cardiac structure in the myocardial wall [4], but there is convincing evidence from DT-MRI data. We present a revisualisation of DT-MRI data and review published DT-MRI results alongside optical, automated

Please cite this article in press as: Gilbert SH, et al., Regional localisation of left ventricular sheet structure: integration with current models of cardiac fibre, sheet and band structure, Eur J Cardio-thorac Surg (2007), doi:10.1016/j.ejcts.2007.03.032

confocal, strain modelling and histological data. Before introducing this analysis a review of the recent literature on mixed sheet populations and sheet merging is presented.

10.2. The evolving concept of myolaminar sheets: mixed sheet populations, sheet merging, the role of sheets in myocardial contraction and inter-individual variability in sheet structure

There is general agreement based upon histology, optical studies and DT-MRI that myocardial fibre orientation is remarkably uniform between and within species [2,13,16,23–25,27,28,30,35–40,44,50,53,54,67–85] (Fig. 3). Intriguingly, there is recent convincing evidence that, despite this fibre structure uniformity, cardiac sheet structure is considerably variable within species [27,44,45].

In order to review the literature on cardiac sheet structure it is first necessary to clarify what is meant by the term 'sheet angle'. This is not a simple task; there are many distinct definitions of sheet angle in the literature. There is no uniformly accepted system for reporting cardiac geometrical data, but cylindrical [39] or prolate spheroidal [57] coordinate systems have been adopted. In either coordinate system, three standard cardiac axes are defined: the long axis, the radial axis and the tangential axis. These axes in turn are used to define three standard cardiac planes: the radial–longitudinal plane, the transverse plane (also known as the short-axis cross-section plane or the radial–circumferential plane) and the tangential plane [81,86]. Sheets have a separate local orthogonal coordinate system defined by the fibre-orientation axis (primary eigenvector), the sheet normal axis (tertiary eigenvector) and a second axis lying in the sheet plane (secondary eigenvector). In general terms, sheet angles relate the local sheet coordinate system to the standard cardiac coordinate system. It is possible to define many different angles between the sheet and cardiac coordinate systems, depending on the chosen plane or axis from each system, and unfortunately no convention has been established. All the sheet angle definitions used in the literature are geometrically dependent, but they are distinct. An additional complication is created by the differing angular scale adopted in reports, being either $0^\circ \leq \beta \leq 180^\circ$ or the equivalent range $-90^\circ \leq \beta \leq +90^\circ$. These considerations make both qualitative and quantitative comparisons of sheet structure between reports difficult.

The definitions of sheet angle adopted in visualisations in this report are those described in general geometric terms by Costa et al. [86], and are defined in relation to the DT-MRI eigenvectors here:

- β'-Sheet angle ($-90^\circ \leq \beta' \leq +90^\circ$): The angle the sheet makes in the longitudinal–radial plane. This is the angle between the transverse plane and the projection of the secondary eigenvector onto the longitudinal–radial plane. Positive angles rise to the heart base from endocardium to epicardium (or LV endocardium to RV endocardium).
- β''-Sheet angle ($-90^\circ \leq \beta'' \leq +90^\circ$): The angle the sheet makes in the transverse plane. This is the angle between the longitudinal–radial plane and the projection of the secondary eigenvector onto the transverse plane.
- βs-Sheet angle ($-90^\circ \leq \beta s \leq +90^\circ$): The angle between the radial axis and the secondary eigenvector lying in the sheet plane (i.e. the projection of the secondary eigenvector onto a standard cardiac plane has *not* been performed). Positive angles rise to the heart base from endocardium to epicardium (or LV endocardium to RV endocardium). This angle is referred to a β by Costa et al. [86], but here we denote it with βs as in Chen et al. [16].

The role, importance and the mechanism of action of cardiac sheets in contraction is addressed in many studies (as presented below) but is still an area of controversy. The cited papers should be referred to for the precise definition of the sheet angle reported. To allow qualitative comparison, angles are reported on the $-90^\circ \leq \beta \leq +90^\circ$ scale and positive sheet angle refers to sheets in which β' rises to the heart base from endocardium to epicardium.

Hort [53–55] proposed a model (Fig. 10 in [53] and Fig. 21 in [3]) to explain wall thinning from systole to diastole in which parallel bundles of fibres are arranged in several stacked layers in systole. In diastole, these layers of like-fibre orientation interdigitate, reducing the number of layers, and allowing the wall to become thinner and the cardiac chambers larger. This model could not function in the presence of cardiac sheets, as it requires bundles of myocytes separated by parallel cleavage planes that, due to their separate connective tissue, can interdigitate during the cardiac cycle.

Spotnitz et al. [46] explored the relative contribution of (i) the myofibre diameter and (ii) the sliding between bundles of myocytes, in myocardial wall thickening. They concluded that (i) changes in fibre thickness could not account alone for the changes in myocardial thickness during contraction, (ii) that 'cleavage planes' were present between groups of myocytes, that (iii) the sliding of groups of myofibres (permitted by cleavage planes between them) was an important mechanism in myocardial contraction, and is evidenced by cleavage planes having a more vertical alignment in diastole and a more horizontal alignment in systole, and that (iv) there is no evidence for insinuation or interleaving of fibres as suggested by Hort. They do not address if cleavage planes separate myolaminae or if they separate bundles of myocytes.

As described above, LeGrice et al. [56] carried out the first quantitative histological analysis of laminar structure throughout the ventricles, and formulated this into a mathematical model [57]. Unlike later reports, this model of the canine ventricles described smoothly varying sheets rather than dual sheet populations; however, regions of abrupt change can be recognised in the data (Fig. 8f). Two canine hearts were studied by histological measurement and two by scanning electron microscopy, but direct heart-to-heart comparisons were not performed. The study reported little detail of inter-individual variability in structure but found significant variation in local sheet structure within hearts, which was considered to be branching from a model of regular transmural endocardial to epicardial planes.

In a mechanics study, LeGrice et al. [43] demonstrated that in dogs >50% of the thickening of the myocardial wall during contraction could be accounted for by slippage along

Please cite this article in press as: Gilbert SH, et al., Regional localisation of left ventricular sheet structure: integration with current models of cardiac fibre, sheet and band structure, Eur J Cardio-thorac Surg (2007), doi:10.1016/j.ejcts.2007.03.032

the cleavage planes between myolaminae. They performed biplane cinematic radiography on radiopaque beads at two cardiac sites in open-chest dogs. The premise for the study was the observation that myocyte thickening alone could account for only a fifth of ventricular wall thickening. This study utilised small regions of the LV anterior free wall and septum from 10 mongrel dog hearts. Inter-individual variation in sheet structure is not recorded in this report.

This work was extended by Costa et al. [44] using the same methodology, who described generally smoothly varying cleavage planes from epicardium to endocardium in three of six dogs, but with abrupt changes associated with the trabeculata–compacta interface (the zone linking trabeculated endocardium and compact subendocardium) in a further three dogs. They confirmed that the laminar nature of the myocardium is critical for normal ventricular dynamics. They also demonstrated that in addition to the sliding of sheets due to interlaminar shear, the sheets participated in myocardial contraction dynamically by extending during systole. They showed the shear component to contribute ~40% and the extension component ~60% to ventricular transmural thickening.

Arts et al. [45] carried out a strain modelling analysis of the data from the above Dokos et al. [58] study and predicted two distinct sheet populations. Histologically determined sheet angles were pooled for all six hearts and revealed a bimodal distribution by cardiac location, of approximately normal sheet orientations. Theoretical modelling of sheet structure using mechanics supported these measurements. They concluded that sheet orientation is not a unique function of the transmural location but occurs in two distinct populations.

Dokos et al. [58] examined laminar shear in samples of excised ventricular myocardium from six pigs. They demonstrated dual cardiac sheet orientations, describing a predominant orientation and an orientation approximately normal to this. They showed that patterns of sheet intersection were not uniform in the circumferential direction, varying significantly over sub-millimetre dimensions. Inter-individual variation in sheet architecture was not characterised or reported.

Jiang et al. [81] produced high-resolution three-dimensional reconstructions of sheet orientation from DT-MRI of the murine heart. They showed whole heart visualisations of sheet angles extracted from the secondary and tertiary eigenvectors (including β'). These images display regional localisations of structure in the LV, but little qualitative and no quantitative descriptions are provided and inter-individual variations are not characterised.

Harrington et al. [11] also identified two sheet populations from a histological study of tissue blocks from the LV interpapillary muscle region of five sheep. They proposed a model with alternating, approximately normal (in the longitudinal–radial plane) positive and negative sheet orientations across the ventricular wall with sheet orientation dependent on transmural depth; positive epicardial, negative mid-myocardial and positive endocardial orientation (Model 5, Fig. 2, part 5). There was relatively little inter-individual variation in sheet orientation (maximum cluster SD = 9 in the reported sheet angle). This model is a satisfactory explanation of the study findings, but is an attempt to extrapolate the features of a small tissue block to a wider region and is hence only valid in a LV without localised heterogeneous aggregations of structure.

Helm et al. [27,83] describe the two sheet populations in DT-MRI data from seven canine hearts. In some LV regions of individual hearts (including the lateral wall) sheets toggled from negative to positive orientation and sometimes back. Combined analysis of sheet orientation from these seven hearts reveals a bimodal distribution of two alternative angle populations. Twenty-five out of 30 selected anatomical regions have such a bimodal distribution (Fig. 8g), having one dominant sheet orientation cluster present in most hearts and one lesser orientation cluster for the remaining hearts. The two sheet populations are approximately normal. The possibility of eigenvector sorting error producing the bimodal distribution was excluded by a *t*-test analysis of the secondary and tertiary eigenvector statistical differences.

Cheng et al. [9] identified two sheet populations in the lateral interpapillary LV muscle region of seven sheep and applied a combined strain modelling and histological method. Sheets were found to exhibit a pleated or accordion-like orientation with alternating sign from subepicardium to subendocardium in a more pronounced manner in the sheep than has been described in the canine by Helm et al. above [27,83]. Intriguingly, they found that systolic fibre shortening was converted to radial wall thickening by a fundamentally different mix of sheet mechanisms at different wall depths. Discontinuities of sheet structure are described at the 20–50% depth and at 50–80% depth with a transmural pleated configuration.

The rat DT-MRI study of Chen et al. [16] demonstrates by DT-MRI the important role played by laminar shear (sheet sliding) in myocardial contraction. This study is similar in approach to Spotnitz et al. [46], but uses DT-MRI in parallel to histology. The presence of sheets of myolaminae (not specifically mentioned by Spotnitz et al.) as well as cleavage planes is confirmed in this study. Separate populations of sheet orientation are not commented upon despite their presence in their DT-MRI results. The paper instead discusses a simple sheet orientation pattern identical to that described by LeGrice et al. [56] – 'positive sheet angles at the base to negative sheet angles at the apex'. The data presentation does not allow analysis of inter-individual sheet variation within groups, but it is noted that significant variability of βs-sheet angle measurements was present. This was explained by (i) DT-MRI resolution limitations voxel averaging over ~20 sheets, (ii) sheet branching and (iii) sorting error of the secondary and tertiary eigenvector.

Rohmer et al. [31] carried out a dual algorithmic extraction and visualisation of fibre structure and sheet structure from one human DT-MRI dataset. The fibre-structure model produced is similar to other published algorithmically extracted fibre maps [28–30]. The sheet model is broadly similar to that proposed by LeGrice et al. [34,43,56,57], with individual concave or convex transmural endocardial to epicardial sheets. Overall, the modelled sheet architecture was complex, with sheet orientation depending on myocardial location. Sheets have greater curvature in the apex. The simple laminar structure model (Fig. 2, part 4) was used as a basis for the development of the sheet reconstruction algorithm, and as such single transmural

Please cite this article in press as: Gilbert SH, et al., Regional localisation of left ventricular sheet structure: integration with current models of cardiac fibre, sheet and band structure, Eur J Cardio-thorac Surg (2007), doi:10.1016/j.ejcts.2007.03.032

sheets with convex/concave surfaces are visualised, and the abutments between separate positive and negative sheet populations are not seen. If this alternative conception of dual positive and negative sheet populations had been applied in algorithm development, the visualisation of sheet structure would not be of continuous warped transmural sheets.

In summary, the literature reveals (i) the two mechanisms by which sheet structure acts as the central mechanism of wall deformation (laminar extension and laminar sliding) and an older, now rejected model of fibre interdigitation, (ii) the existence of two sheet populations with a complex distribution throughout the left ventricle that is somewhat variable between species and (iii) the inter-individual variation in the canine in the distribution of sheet orientation throughout the heart. The inter-individual variation is highly constrained with sheet orientation belonging to clusters. The nature of the boundaries between these sheet populations is poorly understood. Three-dimensional maps of sheet structure throughout the entire ventricle have been published but their features have not been described, nor have they been formalised into models and only limited statistical analysis has been performed. Those studies which have described topological detail of sheet structure have only examined small slabs of the lateral left ventricle, with emphasis on sheet changes between systole and diastole [16] and in cardiac disease [13,24].

10.3. A novel description of canine left ventricular tertiary structure

The data acquired by Helm et al. and Beg et al. [13,26,27,83] have been extended into a comprehensive resource of cardiac DT-MRI data available from the Centre for Cardiovascular Biomechanics and Modelling (CCBM; http://www.ccbm.jhu.edu/index.php). We revisualised these data alongside DT-MRI data from three mongrel dog hearts, acquired and pre-processed by Hsu et al. [35], then at the Center for In Vivo Microscopy, Duke University Medical Center.

As discussed, Helm et al. [83] provide a description of bimodal populations (Fig. 8g) of sheet orientation when ventricular regions are compared between dogs by cardiac location. Although visualisations are presented in these reviewed studies, these are not comprehensive and do not explore the variable distribution of cardiac structure in different canine hearts, or how this bimodal angle distribution is distributed throughout individual hearts in three dimensions. A hypothesis was formed on the basis of the findings of Helm et al. [83] that (i) bimodal distributions of sheet orientation, (ii) other observations on sheet structure in the literature and (iii) consistently varying fibre helix angles in all studied hearts: cardiac sheet structure can belong to a range of structural forms, with the smooth separation of bimodal peaks indicating a distribution of form, rather than two or more distinct structural models. The range of forms adopted by sheet structure is constrained by the myocyte fibre orientation (as these cells course through the sheets) which has a uniform helical organisation in the left ventricle.

In order to investigate this hypothesis we have revisualised the sheet orientation from selected basal, equatorial and apical slices from 12 normal canine hearts (Fig. 7a). Established DT-MRI visualisation methods [83] and tools were applied to this public domain data and anatomical views were selected to provide a comprehensive presentation of sheet architecture in three dimensions in individual hearts. The visualisations presented are of the β'-sheet angle and the angular scale $-90^\circ \leq \beta' \leq +90^\circ$ is adopted. The sheet structures in visualised short axis slices are described.

The structural continuity within individual hearts underlying the bimodal sheet orientation described above can be seen. Some hearts (8, 6, 16, 12, 11) have predominant β'-sheet angles greater than 22.5° or less than 22.5° ($-22.5 > \beta' > +22.5$) with relatively little in short-axis plane sheet orientation (henceforth referred to as SA-planar). Other hearts have larger areas of SA-planar ($-22.5 < \beta' < +22.5$) β'-sheet angle (9, 15, 13, 10, A, C and B).

Eleven hearts (9, 15, 13, 10, 8, 6, 16, 11, 12, A and C) have predominantly negative β'-sheet angle in the LV equatorial posterior region, with one heart (B) having predominantly positive β'-sheet angle in this zone. The equatorial anterolateral LV free wall is predominantly planar in four (9, 15, 10 and B), negative in four (13, 8, 6, 11) and positive in four (16, 12, A and C) hearts.

β' in the basal anterior LV free wall is positive in ten (9, 15, 13, 10, 8, 16, 12, A and C), mixed in one (10), negative in one (B) and planar in one (6) heart.

The three-dimensional cut out slab (Fig. 8e) shows that described regions of confluent positive (red) or negative (blue) sheet angulation are continuous stacks in three dimensions. The green SA-planar areas also form contiguous regions merging more gradually with red and blue stacks. It is inappropriate to describe these features as bands – they are best interpreted as stacks of similar sheet orientation, reminiscent of a stack of angled books.

This variability in sheet structure is far from random. As noted above and in Helm et al. [83], sheet angles belong to two populations following a bimodal distribution with average peaks at 45.5° and 117.6° (equivalent to −44.5° and 27.6° on β'-sheet angle scale adopted here, see Fig. 8g). Sheet structure is present as circumferentially confluent zones of near-continuous orientation, often having sharp terminations. Regions of positive and negative β'-sheet angle often run adjacently in the circumferential direction with sudden angular change at their abutments. In other cardiac regions sheets more gently merge into each other.

As such, positive and negative sheet stacks are not features of a regularly undulating continuum of sheet structure. This is demonstrated by the sheet orientation 10° contour map in Fig. 8b, which shows that abutting red and blue confluent sheet zones have very steep angular change between them. It should also be noted that, although this angular change is steep, it is not discontinuous; they represent regions of rapid orientation change with distance (Fig. 8b, iii).

Three hearts (15, 16, 11), representative of the principal sheet features of the continuum of structure, are visualised in three dimensions in Fig. 8a. The apex of heart 15 has an inner ring of positive sheets encircled by an outer ring of negative β'-sheet angle. At the apical origin of the LV

Please cite this article in press as: Gilbert SH, et al., Regional localisation of left ventricular sheet structure: integration with current models of cardiac fibre, sheet and band structure, Eur J Cardio-thorac Surg (2007), doi:10.1016/j.ejcts.2007.03.032

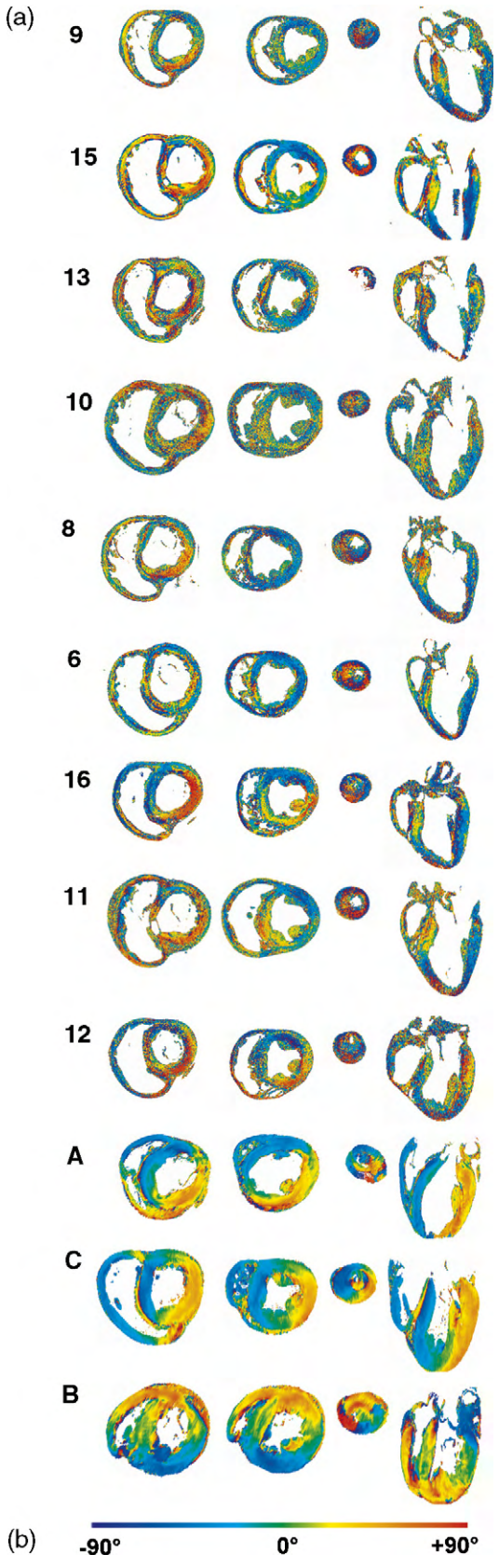

Fig. 7. Reconstruction of canine ventricular β'-sheet angle. β'-sheet angle has been defined as the angle between the transverse plane and the projection of the secondary eigenvector onto the radial plane [81]. Positive β'-sheet angles rise to the heart base from endocardium to epicardium (or LV endocardium to RV endocardium). (a) β'-sheet angle maps from three-dimensional reconstruction of DT-MRI for 12 normal canine hearts. Numbered hearts are from datasets, courtesy of Patrick Helm and Raimond Winslow et al. at The Center for Cardiovascular Bioinformatics & Modeling and Elliot McVeigh at the National Institute of Health. Data for hearts denoted by capital letters were acquired from Hsu et al. [35], then at the Center for In Vivo Microscopy, Duke University Medical Center. A top view of basal, equatorial and apical slices (left to right) is shown alongside an approximately anterior view of a mid-heart slice. The hearts are ordered by eye so as to demonstrate a distribution of changing β'-sheet angle properties from heart 9 (top) to heart 11 (bottom). (b) β'-sheet angle scale bar from +90° red to −90° blue.

papillary muscles the negative sheet population has dominated the positive population. Basal to this, at the basal extent of the papillary muscles, positive sheets dominate the anterior LV, while negative sheets dominate the posterior LV. In the basal LV, overall positive sheet predominates.

Heart 16 (Fig. 8a) has a similar overall LV architecture but has significantly greater positive β'-sheet angle in the anterior LV throughout the equatorial zone.

In heart C (Fig. 8a) positive β'-sheet angle extends from the equatorial zone to the apical zone, where positive and negative sheets are both present.

Fig. 8c and d is a visualisation of posterior view of heart 15, showing β'-sheet angle. It should be noted that the underlying sheet structure is similar to that described for the HVMB in Fig. 4.

Fig. 8f shows a top view of an equatorial LV slice of histologically derived sheet orientation. The data are derived from LeGrice et al. [27]. The β'-sheet angle orientation shown is not identical to any of the 12 canine hearts in Fig. 7a but fits into the continuum of structure being intermediate between hearts 12 and B.

10.4. Discussion of sheet stacks

How do the described stacks of laminar structure fit into the general cardiac sheet literature? All the sheet structural features described in the reviewed literature — two populations [9,11,13,27,44,45,58,83], toggling positive/negative accordion pattern [11,27], patches [45], smoothly varying and abrupt changes [44,58], inter-individual variation of sheet orientation with a bimodal distribution [27,45,83] — can be accommodated by the restrained structural continuum model proposed here.

The sheet stacks described in this study are often clearly defined. Sheet reconstructions showing the same general pattern stacks have been published for the dog (Figs. 7 and 8) [27], mouse [81], rabbit [27] and rat [16], but without explicit descriptive identification of structures analogous to our stacks. Crescent-shaped stacks are visible in the murine DT-MRI sheet reconstruction of Jiang et al. [81], similar in morphology to those visualised here.

The rat study of Chen et al. [16] reveals prominent abutting positive and negative sheet stacks; however, these have differences in conformation to those described here for the dog. There are no SA-planar regions reported, rather overlapping crescents of opposite polarity (Fig. 6e). The boundary zones between positive and negative stacks are very sharp, suggesting a sudden change of orientation.

Some of the sheet features described in this review are present in the registered canine DT-MRI visualisations of

Please cite this article in press as: Gilbert SH, et al., Regional localisation of left ventricular sheet structure: integration with current models of cardiac fibre, sheet and band structure, Eur J Cardio-thorac Surg (2007), doi:10.1016/j.ejcts.2007.03.032

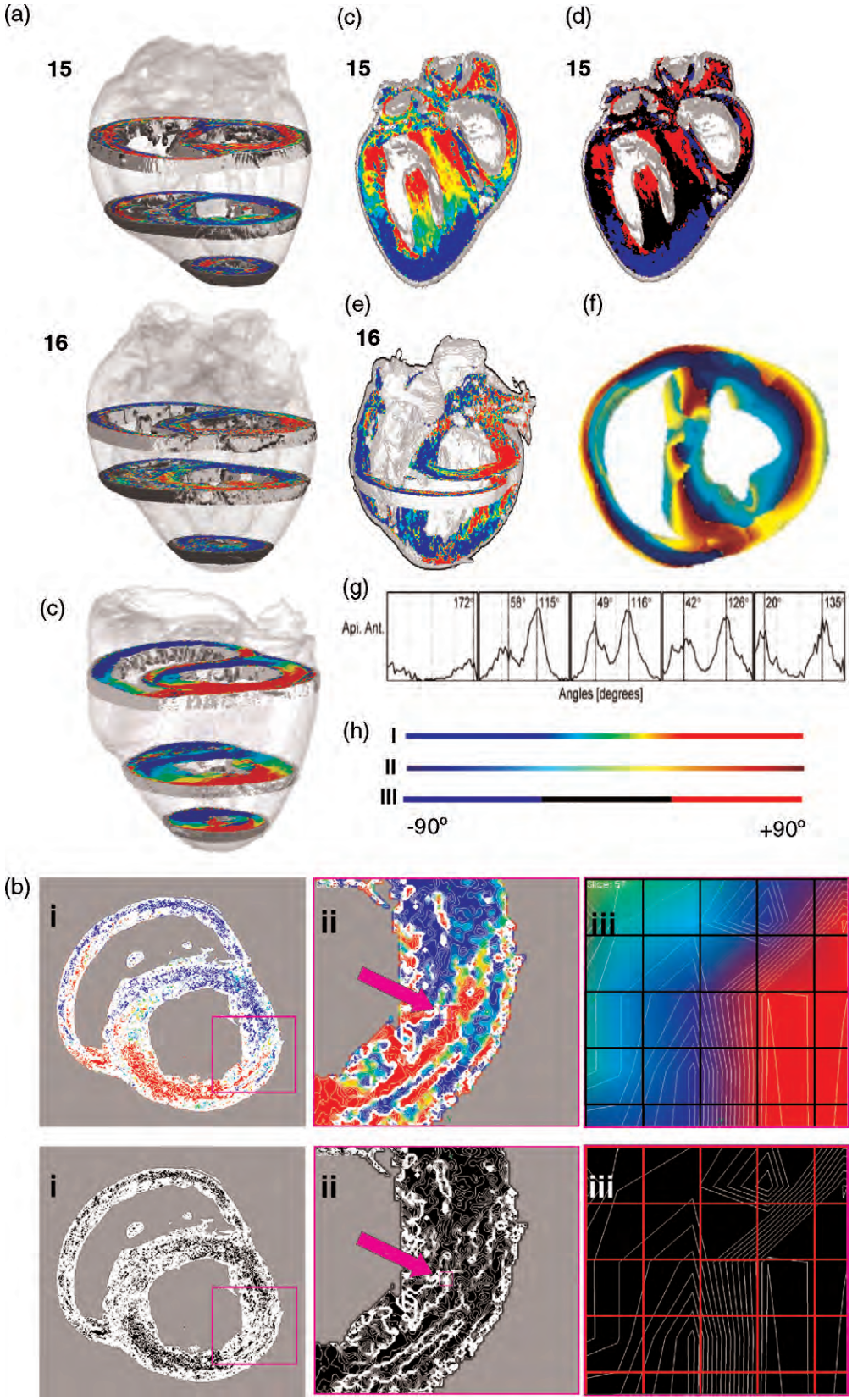

Fig. 8. (a) Anterior view of three-dimensional detailed representation of β'-sheet angle from hearts 15 (top), 16 (middle) and C (bottom) showing detail of sheet morphology in three dimensions. Basal, equatorial and apical slices are shown from these three hearts, which represent major forms within the continuum of cardiac structure. β'-sheet angle is coloured as shown in the scale bar I (h) from +90° red to −90° blue. (b) Top view of short axis cross-section of lateral LV free wall of heart 16. In the top panel β'-sheet angle is coloured as shown in the scale bar I (h) from +90° red to −90° blue, in the bottom panel a cardiac outline is shown in black with no

Please cite this article in press as: Gilbert SH, et al., Regional localisation of left ventricular sheet structure: integration with current models of cardiac fibre, sheet and band structure, Eur J Cardio-thorac Surg (2007), doi:10.1016/j.ejcts.2007.03.032

Helm et al. [13], but certain features are more pronounced while others are more subtle. This is likely to be a consequence of the data registration and image averaging methodology utilised. This algorithmic methodology combines data from several heart DT-MRI scans into a single spatially registered and combined *average* visualisation of sheet structure. This emphasises features with fixed presence between hearts, and smoothes out those that have a more variable presence between individuals. Given the described bimodal angle population present between individuals [27,83] and the visualisation presented here the application of such methods to cardiac sheet structure data is likely to be of limited value.

10.5. Cardiac sheet structure features, pinnation, fibre paths and the HVMB

The described sheet structures are related in location, although not coincident, with the DT-MRI primary eigenvector transitions (Fig. 5a–d). The precise relationship between the DT-MRI determined sheet features and the histologically described pinnation features of Hort [54] (Fig. 5e and f) cannot be determined without further studies, as the histological features are from hearts of unknown sheet structure. As they all form part of the same complex continuum of structure, these features must be related.

11. Sheet stack boundaries

11.1. The nature of sheet stack boundaries

The DT-MRI data provide a picture of global sheet behaviour throughout the ventricles. Due to resolution limitations (discussed in detail below) little information is provided about the nature of sheet interactions at stack boundaries.

The nature of these boundaries is best studied by high-resolution three-dimensional confocal microscopy. Two such studies [20,21] have analysed lateral LV transmural tissue blocks from rats (producing the data shown in Fig. 6a–c). These reports have focused on technique validation for use in electrical modelling [87], rather than the anatomical structure revealed. Detailed study of the microstructural architecture in Fig. 6 and the video from which these images were extracted reveals intriguing and unreported detail of myolaminar architecture.

Two sheet populations can be seen to co-exist in the same slab of tissue. A highly intricate but ordered pattern of sheet merging is observed, with $\beta' \sim +45^\circ$ and $\beta' \sim -45^\circ$ myolaminae coalescing on myolaminae of rhomboid cross-section in the mid-myocardium. These rhomboid structures appear to carry the circumferential fibres [4,48] (as described in Model 3 [48]). Merging is subtle, and working back from the rhomboid central zone, two sheet populations can be seen to co-exist simultaneously in the same region (Fig. 6b and c, blue circles). On moving towards the epicardium or endocardium, the positive or negative sheet orientation dominates.

The detail of the sheet interactions is best considered in the light of the rat global sheet architecture as revealed from DT-MRI (Fig. 6e). These DT-MRI data are from a different rat (and a different research group) but the same sheet features are revealed (negative endocardial sheets meeting positive epicardial sheets). In the transition zone, yellow sheet orientation (almost SA-planar, βs $\sim 15^\circ$) is recorded.

No detailed confocal data are currently available for the canine, so the nature of the boundaries between the $\beta' \sim \pm 45$ sheet stacks and the transverse $\beta' \sim 0^\circ$ sheet stacks is unknown. There may be a similar pattern of merging with co-dominance at the stack boundaries, or this may be limited to the intersection regions between positive and negative $\beta' \sim \pm 45^\circ$ sheet stacks, with a more gradual change of a single sheet population in the rest of the myocardium.

11.2. Role of stack interaction boundaries (positive to negative sheet stack abutments)

No investigations of the role sheet merging across stack boundaries have been undertaken. Given the complex merging of laminae across these boundaries it is possible that sheet sliding and extension is continuous across this zone but with the changing of the direction of strain. It is possible that the loose structure of the merging zone between positive and negative sheets, with the rhomboid myolaminae which resemble bundles of myocytes, may allow the interdigitation proposed by Hort [53–55] as a mechanism of myocardial thickness change between systole and diastole. This interleaving would not be possible in regions of confluent sheets (predominant positive or negative orientation, towards the epicardium and endocardium of Fig. 6a–c). Interleaving was not observed by Spotnitz et al. [46], but their study concentrated on regions of confluent cleavage planes, and they did not discuss dual populations of cleavage planes (despite their presence in their data), and as such they could

sheet angle colouration. The panel shows an image of scanned dimensions 80 mm × 80 mm and 256 voxels × 256 voxels. 10° contours (in white) have been applied to the cut surface, which in (b, i top) are spread out over the red and blue zones of similar β'-sheet angle but are crowded together (forming a thick white line) at the boundaries between these zones. The purple square shown in (b, i) is magnified to the right (b, ii – scanned dimensions 28 mm × 28 mm, 90 voxels × 90 voxels) and shows greater detail of the contours in positive to negative sheet boundaries. The small purple square (indicated by the arrow) is magnified to the right in (b, iii – scanned dimensions 1.4 mm × 1.4 mm, 4.5 voxels × 4.5 voxels) where detail of the contours (angular change) can be seen in a small region of the myocardial wall. The grid overlying (b, iii) shows the voxel dimensions (voxels are 0.3125 mm × 0.3125 mm in this plane). As seen in the top panel angular values are interpolated between voxels. At this scale it can be seen that the change from negative to positive sheet orientation takes place between two adjacent voxels. (c and d) Posterior long-axis three-dimensional view of heart 15 with β'-sheet angle is coloured as shown in the scale bar I in (c) and scale bar III in (d) from +90° red to −90° blue. This view clearly shows that the three-dimensional morphology of myocardial sheets recreate the band segments of the HVMB as described in Fig. 4. (e) Three-dimensional visualisation of heart 16 β'-sheet angle shows that the contiguous zones of similar β'-sheet angle are continuous in three dimensions, and hence can be considered as stacks of laminae of the same orientation. (f) Top view of data from a histological sheet angle reconstruction of canine heart presented by Scollan et al. [36], used with permission, from the data of LeGrice et al. [56]. The inclination angle of the tertiary eigenvector in the tangential plane (a measure which, similar to β', gives the base–apex orientation of the cardiac sheets) is coloured as shown in the scale bar II (i) from +90° red to −90° blue. (g) Sample of data from 5 of a total of 30 anatomical regions in seven canine hearts from Fig. 8 in Helm et al. [43], used with permission, showing the bimodal distribution of sheet angle with the average peak sheet angles (for all the data) at 45.5° and 117.6° (equivalent to −44.5° and 27.6° on β'-sheet angle scale adopted in the visualisations presented here). (h) Colour scale bars used throughout this figure.

Please cite this article in press as: Gilbert SH, et al., Regional localisation of left ventricular sheet structure: integration with current models of cardiac fibre, sheet and band structure, Eur J Cardio-thorac Surg (2007), doi:10.1016/j.ejcts.2007.03.032

have missed this finding. Indeed, such thickening of myocyte bundles and obliteration of cleavage planes may be observed in the positive to negative cleavage plane abutment to the left of Plate 2 in [46] (note that the myocardial images in this plate are aligned images from different fixed rat hearts).

The junctional region may act as region of meeting of forces with the sheet populations acting antagonistically and/or to stabilise each other, as explored by Sengupta et al. [88]. During isovolumic contraction, shortening of subendocardial myofibres is accompanied by stretching (and hence stiffening) of subepicardial fibres. These authors hypothesise that this could form a functional analogue of the 'rigid external cylinder' proposed by Torrent-Guasp et al.

12. Technical limitations of techniques

12.1. Technique focus

It is tempting to view the data produced from novel imaging techniques as unbiased, absolute and definitive – not as artefact-prone and subject to investigator bias as with traditional techniques. However, equal care is needed in the interpretation of these data – its weakness can be that it seems to produce all the answers. In fact, each imaging technique has a *focus* – a level of structure which it reveals – and in so doing it can obscure higher- and lower-order structure. Confocal imaging of tissue blocks has revealed detailed laminar structure and cross-meshing, but obscures overall sheet patterns and predominant fibre orientation. Primary eigenvector fibre angles and optical polarisation maps reveal primary fibre trajectory but obscure local branching and hide sheet structure. Indeed, DT-MRI reports presenting only the primary eigenvector (principal fibre orientation) have been used to argue against regional structural differences within the ventricles [30].

12.2. DT-MRI: resolution

There are technical reasons for the *focus* of each technique. The resolution of DT-MRI applied to cardiac studies has generally been approximately 300 μm within slices and 1000 μm between slices [30,35–40]. This is not sufficient to depict the finer structure of myocardial laminae [16] (of dimension ~50 μm in dog [56]). The measured β'-sheet angle reported in each DT-MRI voxel will be an averaging of ~6–20 sheets. As discussed, this has implications for the power of DT-MRI to resolve sheet behaviour at stack boundaries. At current resolution it produces a schema of locally averaged sheet direction – so results should be interpreted in this light.

12.3. DT-MRI: eigenvector sorting

In DT-MRI processing, sheet angle is calculated from the secondary eigenvector and sheet normal from the tertiary eigenvector. These values are sorted by magnitude, the secondary always being greater than the tertiary. It has been hypothesised that an eigenvector-sorting problem could occur where secondary and tertiary are similar in magnitude [25,83], and that this could invalidate determined sheet angles. A statistical analysis by Helm et al. [83] addressed this question and concluded that sorting was robust to this error, but the study did not consider sheet co-dominance in regions of sheet merging. Analysis of the microstructural detail of sheet features in confocal data reveals that the true structure consists of complex sheet merging with co-dominance of positive and negative sheets, while in DT-MRI data this is represented by ~SA-planar sheet conformation. An implication is that histological confirmation of detail of sheet structure is required, and that this should be incorporated with the statistical analysis of DT-MRI data to allow identification of co-dominant sheet areas. The canine histological sheet orientation data (Fig. 8f) provide some validation and show that the gross patterning, if not the local microstructural detail, of sheet features is robust to sorting artefact.

12.4. Confocal microscopy: fixation artefact

Tseng et al. [25] described considerable distortion of myolaminae orientation between ink prints from un-fixed tissue and histological measurements after fixation and sectioning. It is likely that the cleavage planes in Fig. 6a–c have opened up due to shrinkage and dehydration in the fixation process.

12.5. Confocal microscopy: real myolaminae and artefact myolaminae

There has been some debate about the presence of myolaminae and their structure. Harrington et al. [11] divided planes present in sectioned fixed tissue into true laminae (the predominant sheet orientation visible on the sectioned frozen tissue surface and on un-sectioned tissue) and artefact. On placing the tissue on a slide, gaps opened up dividing the tissue into laminae along the visible sheet orientation over a period of 3 min. On observing the sections for longer periods, additional gaps opened up, which they described as cracks and dehydration artefact. Are any of the sheet-merging features described in Fig. 6 artefact? This is unlikely – the rat hearts were embedded in epoxy resin after fixation, fixation is not known to produce crack artefacts, and cracking of the epoxy resin block on sectioning would be grossly visible, would produce optical distortion and would not occur along planes of equal thickness matching known myolaminae width (four to six fibres). It is also unlikely that perpendicular planes would be created, meeting so regularly on rhomboid myolaminae. It is possible that some of the cracking observed by Harrington et al. [11] were real cleavage planes opening up, or that that much greater care is needed with frozen tissue than fixed tissue.

These technical problems highlight the need for an intelligent integration of results from the different techniques, building together of schema of heart structure to form a united concept of cardiac architecture.

13. Validity of the proposed sheet stack structure by Grant's principles

In drawing together a novel description of cardiac structure one risks clouding the debate rather than clarifying

Please cite this article in press as: Gilbert SH, et al., Regional localisation of left ventricular sheet structure: integration with current models of cardiac fibre, sheet and band structure, Eur J Cardio-thorac Surg (2007), doi:10.1016/j.ejcts.2007.03.032

it. To avoid this it is necessary to place the model in a clear context of the known structural facts and the principles as outlined by Grant. An important component in this is to consider the technical limitations and possible artefact due to experimental method.

As evidenced by the contour and microstructural description of boundary zones between sheet stacks, the new model fits into the principle of a syncytial myocardial community. It is also appreciated that the sheet structure obtained from DT-MRI secondary eigenvector data is only one level on which the myocardium can be approached — and that other valid approaches reveal *no* discernable detail of sheet structure (see the primary eigenvector fibre orientation data of Fig. 3). In this sense the sheet structure is best viewed as a schema of one level of cardiac structure — whole heart sheet behaviour, underlying the higher-order schema of predominant fibre direction and overlying the schema of local myolaminar meshing. The DT-MRI technique is inherently statistical and of uniform bias across the entire structure. The β'-sheet angle maps (Fig. 8) clearly demonstrate the described sheet features. A complete statistical analysis of the stack structures from grouped hearts and across species is required, but this preliminary analysis demonstrates that Grants' criterion of statistical uniqueness is likely to be satisfied. Debate on whether the sheet stacks described are a schema of cardiac structure or distinct *anatomical bundles* (as described by Grant) is largely semantic. Addressing whether the stacks constitute unique *physiological bundles* is also a naive approach. It is more useful to address the role played by interaction of these ubiquitous, intricately intermeshed structures in cardiac excitation and contraction.

14. Implications

The distribution and merging pattern of the sheet populations lead to many questions to be answered by future directed research. What are the sheet sliding (shear) and sheet extension implications for the sheet stack merging pattern? Is the heterogeneity of myocardial action potential morphology [89] related to sheet populations rather than simple transmural or base–apical ventricular location?

Yet, more questions are raised by the heterogeneity of cardiac sheet structure between dogs. Reviewed evidence points to the critical role of sheets in myocardial contraction, so how do such different structures act to produce the same function? Are some sheet conformations more efficient, more resistant to myocardial failure or of different electrical conduction and arrythmogenesis potential? Do inbred populations such as laboratory rats and mice have more uniform cardiac sheet structure, as suggested by the data in Spotnitz et al. [46]? Do dogs having perhaps the greatest body form heterogeneity of any domesticated species (due to selective breeding and paedomorphosis [90]) also have much greater cardiac heterogeneity than man or pigs? Does the maintenance of such a regular fibre angle distribution despite β'-sheet angle heterogeneity reflect a greater importance of fibre angle than sheet orientation in myocardial contractile function, contrary to evidence in the reviewed literature?

The recent demonstration of sheets in echocardiography [88] may provide a methodology to study the dynamics of sheet interaction throughout the cardiac cycle, particularly if sheets can be visualised in three-dimensional ultrasound images.

The cardiac topology as described by Torrent-Guasp et al., although reflecting some genuine features of heart structure, is a schema of minor importance and is unlikely to have physiological consequences. It does not apply equally to all canine individuals and may not apply equally in other species.

Fibre orientation and sheet architecture are known to be important in cardiac contraction [16,44,91] and are remodelled in cardiac disease [13,24,85,92]. The importance of sheet stacks described in this review has not been studied, nor has their alteration in cardiomyopathy. Given the known importance of sheets in cardiac contraction it is likely that sheet stacks will also be functionally important, particularly the sharp orientation changes at boundaries between positive and negative sheets.

15. Conclusions

The novel description of cardiac sheet stacks in this review is compatible with the published histological and DT-MRI reports of dual sheet populations and inter-individual variability of sheet structure.

Greenbalm et al. [50] concluded that there was a complex regional variation in left ventricular structure, that modelling based on uniform wall structure could not explain wall movement and that traditional dissection techniques and histology would be inadequate to fully characterise possible regional difference in LV arrangement.

New imaging technologies allow greater characterisation of regional differences, but the application of this knowledge to modelling wall movement and guiding surgery is in its infancy.

This report of sheet structure describes the overall pattern in the left ventricle as revealed by the DT-MRI secondary eigenvector and confocal microscopy. It does not constitute a finalised complete model of cardiac structure, but features described here must be incorporated into any future such model.

Note on images: All short-axis (cross-section) cardiac views are presented as top views looking towards the cardiac apex.

Acknowledgements

The canine ventricular DT-MRI datasets presented in Figs. 3, 5 and 7 were acquired and pre-processed by Hsu et al. [35], then at the Center for In Vivo Microscopy, Duke University Medical Center, and the datasets presented in Fig. 8 were acquired and pre-processed by Patrick Helm and Raimond Winslow et al. at The Center for Cardiovascular Bioinformatics & Modeling and Elliot McVeigh at the National Institute of Health.

References

[1] Criscione JC, Rodriguez F, Miller DC. The myocardial band: simplicity can be a weakness. Eur J Cardiothorac Surg 2005;28:363.

[2] Grant RP. Notes on the muscular architecture of the left ventricle. Circulation 1965;32:301–8.
[3] Streeter Jr DD. Gross morphology and fiber geometry of the heart. Baltimore: Williams and Wilkins; 1979. p. 61–112.
[4] Anderson RH, Ho SY, Redmann K, Sanchez-Quintana D, Lunkenheimer PP. The anatomical arrangement of the myocardial cells making up the ventricular mass. Eur J Cardiothorac Surg 2005;28:517–25.
[5] Gerdes AM, Moore JA, Hines JM, Kirkland PA, Bishop SP. Regional differences in myocyte size in normal rat heart. Anat Rec 1986;215:420–6.
[6] Satoh H, Delbridge LM, Blatter LA, Bers DM. Surface:volume relationship in cardiac myocytes studied with confocal microscopy and membrane capacitance measurements: species-dependence and developmental effects. Biophys J 1996;70:1494–504.
[7] Spach MS, Heidlage JF, Barr RC, Dolber PC. Cell size and communication: role in structural and electrical development and remodeling of the heart. Heart Rhythm 2004;1:500–15.
[8] Kocica MJ, Corno AF, Carreras-Costa F, Ballester-Rodes M, Moghbel MC, Cueva CNC, Lackovic V, Kanjuh VI, Torrent-Guasp F. The helical ventricular myocardial band: global, three-dimensional, functional architecture of the ventricular myocardium. Eur J Cardiothorac Surg 2006;29:S21–40.
[9] Cheng A, Langer F, Rodriguez F, Criscione JC, Daughters GT, Miller DC, Ingels Jr NB. Transmural sheet strains in the lateral wall of the ovine left ventricle. Am J Physiol Heart Circ Physiol 2005;289:H1234–41.
[10] McDevitt TC, Angello JC, Whitney ML, Reinecke H, Hauschka SD, Murry CE, Stayton PS. In vitro generation of differentiated cardiac myofibers on micropatterned laminin surfaces. J Biomed Mater Res 2002;60:472–9.
[11] Harrington KB, Rodriguez F, Cheng A, Langer F, Ashikaga H, Daughters GT, Criscione JC, Ingels NB, Miller DC. Direct measurement of transmural laminar architecture in the anterolateral wall of the ovine left ventricle: new implications for wall thickening mechanics. Am J Physiol Heart Circ Physiol 2005;288:H1324–30.
[12] Entcheva E, Bien H. Tension development and nuclear eccentricity in topographically controlled cardiac syncytium. Biomed Microdevices 2003;5:163.
[13] Helm PA, Younes L, Beg MF, Ennis DB, Leclercq C, Faris OP, McVeigh E, Kass D, Miller MI, Winslow RL. Evidence of structural remodeling in the dyssynchronous failing heart. Circ Res 2006;98:125–32.
[14] Anderson RH, Ho SH, Sanchez-Quintana D, Redmann K, Lunkenheimer PP. Heuristic problems in defining the three-dimensional arrangement of the ventricular myocytes. Anat Rec Part A 2006;288A:579–86.
[15] Fernandez-Teran MA, Hurle JM. Myocardial fiber architecture of the human heart ventricles. Anat Rec 1982;204:137–47.
[16] Chen J, Liu W, Zhang H, Lacy L, Yang X, Song SK, Wickline SA, Yu X. Regional ventricular wall thickening reflects changes in cardiac fiber and sheet structure during contraction: quantification with diffusion tensor MRI. Am J Physiol Heart Circ Physiol 2005;289:H1898–907.
[17] Caulfield JB, Borg TK. The collagen network of the heart. Lab Invest 1979;40:364–72.
[18] Torrent-Guasp F, Ballester M, Buckberg GD, Carreras F, Flotats A, Carrio I, Ferreira A, Samuels LE, Narula J. Spatial orientation of the ventricular muscle band: physiologic contribution and surgical implications. J Thorac Cardiovasc Surg 2001;122:389–92.
[19] Fox CC, Hutchins GM. The architecture of the human ventricular myocardium. Johns Hopkins Med J 1972;130:289–99.
[20] Young AA, Legrice IJ, Young MA, Smaill BH. Extended confocal microscopy of myocardial laminae and collagen network. J Microsc 1998;192:139–50.
[21] Sands GB, Gerneke DA, Hooks DA, Green CR, Smaill BH, Legrice IJ. Automated imaging of extended tissue volumes using confocal microscopy. Microsc Res Tech 2005;67:227–39.
[22] McLean M, Prothero J. Myofiber orientation in the weanling mouse heart. Am J Anat 1991;192:425–41.
[23] Jouk PS, Usson Y, Michalowicz G, Grossi L. Three-dimensional cartography of the pattern of the myofibres in the second trimester fetal human heart. Anat Embryol 2000;202:103–18.
[24] Chen J, Song SK, Liu W, McLean M, Allen JS, Tan J, Wickline SA, Yu X. Remodeling of cardiac fiber structure after infarction in rats quantified with diffusion tensor MRI. Am J Physiol Heart Circ Physiol 2003;285:H946–54.
[25] Tseng WY, Wedeen VJ, Reese TG, Smith RN, Halpern EF. Diffusion tensor MRI of myocardial fibers and sheets: correspondence with visible cut-face texture. J Magn Reson Imaging 2003;17:31–42.
[26] Beg MF, Helm PA, McVeigh E, Miller MI, Winslow RL. Computational cardiac anatomy using MRI. Magn Reson Med 2004;52:1167–74.
[27] Helm P, Beg MF, Miller MI, Winslow RL. Measuring and mapping cardiac fiber and laminar architecture using diffusion tensor MR imaging. Ann N Y Acad Sci 2005;1047:296–307.
[28] Zhukov L, Barr AH. Heart-muscle fiber reconstruction from diffusion tensor MRI. In: Proceedings of the 14th IEEE visualization 2003 (VIS'03). IEEE Computer Society; 2003.
[29] Kondratieva P, Kruger J, Westermann R. The application of GPU particle tracing to diffusion tensor field visualization. In: Proceedings IEEE visualization 2005.
[30] Schmid P, Jaermann T, Boesiger P, Niederer PF, Lunkenheimer PP, Cryer CW, Anderson RH. Ventricular myocardial architecture as visualised in postmortem swine hearts using magnetic resonance diffusion tensor imaging. Eur J Cardiothorac Surg 2005;27:468–72.
[31] Rohmer D, Sitek A, Gullberg GT. Reconstruction and visualization of fiber and sheet structure with regularized tensor diffusion MRI in the human heart. Lawrence Berkeley National Laboratory Publication. LBNL-60277, 2006.
[32] Chen M, Clayton RH, Holden AV, Tucker JV. Constructive volume geometry applied to visualisation of cardiac anatomy and electrophysiology. Int J Bifurcat Chaos 2003;13.
[33] Chen M, Clayton RH, Holden AV, Tucker JV. Visualising cardiac anatomy using constructive volume geometry. In: Magnin IE, Montagnat J, Clarysse P, Nenonen J, Katila T, editors. Functional imaging and modelling of the heart. Lyon, France: Springer; 2003. p. 30–8.
[34] LeGrice I, Hunter P, Young A, Smaill B. The architecture of the heart: a data-based model. Philos T Roy Soc A 2001;1217–32.
[35] Hsu EW, Muzikant AL, Matulevicius SA, Penland RC, Henriquez CS. Magnetic resonance myocardial fiber-orientation mapping with direct histological correlation. Am J Physiol 1998;274:H1627–34.
[36] Scollan DF, Holmes A, Winslow R, Forder J. Histological validation of myocardial microstructure obtained from diffusion tensor magnetic resonance imaging. Am J Physiol 1998;275:H2308–1.
[37] Scollan DF, Holmes A, Zhang J, Winslow RL. Reconstruction of cardiac ventricular geometry and fiber orientation using magnetic resonance imaging. Ann Biomed Eng 2000;28:934–44.
[38] Hsu EW, Henriquez CS. Myocardial fiber orientation mapping using reduced encoding diffusion tensor imaging. J Cardiov Magn Reson 2001;3:339–48.
[39] Geerts L, Bovendeerd P, Nicolay K, Arts T. Characterization of the normal cardiac myofiber field in goat measured with MR-diffusion tensor imaging. Am J Physiol Heart Circ Physiol 2002;283:H139–45.
[40] Hsu EW. Myocardial fiber orientation mapping via MR diffusion tensor imaging. In: Joint EMBS-BMES conference. Houston, TX: IEEE; 2002. p. 1169–70.
[41] Peskin CS. Fiber architecture of the left ventricular wall: an asymptotic analysis. Commun Pur Appl Math 1989;42:79–113.
[42] Torrent-Guasp F. The cardiac muscle. Madrid: Juan March Foundation Ltd.; 1973.
[43] LeGrice IJ, Takayama Y, Covell JW. Transverse shear along myocardial cleavage planes provides a mechanism for normal systolic wall thickening. Circ Res 1995;77:182–93.
[44] Costa KD, Takayama Y, McCulloch AD, Covell JW. Laminar fiber architecture and three-dimensional systolic mechanics in canine ventricular myocardium. Am J Physiol 1999;276:H595–607.
[45] Arts T, Costa KD, Covell JW, McCulloch AD. Relating myocardial laminar architecture to shear strain and muscle fiber orientation. Am J Physiol Heart Circ Physiol 2001;280:H2222–9.
[46] Spotnitz HM, Spotnitz WD, Cottrell TS, Spiro D, Sonnenblick EH. Cellular basis for volume related wall thickness changes in the rat left ventricle. J Mol Cell Cardiol 1974;6:317–31.
[47] Clayton RH. Computational models of normal and abnormal action potential propagation in cardiac tissue: linking experimental and clinical cardiology. Physiol Meas 2001;22:R15–34.
[48] Rushmer RF, Crystal DK, Wagner C. The functional anatomy of ventricular contraction. Circ Res 1953;1:162–70.
[49] Krehl L. Beiträge zur Kenntnis der Füllung und Entleerung des Herzens. Abh Math-Phys Kl Saechs Akad Wiss 1891;17:341–62.
[50] Greenbaum RA, Ho SY, Gibson DG, Becker AE, Anderson RH. Left ventricular fibre architecture in man. Br Heart J 1981;45:248–63.
[51] Sanchez-Quintana D, Garcia-Martinez V, Hurle JM. Myocardial fiber architecture in the human heart. Anatomical demonstration of modifications in the normal pattern of ventricular fiber architecture in a malformed adult specimen. Acta Anat (Basel) 1990;138:352–8.

Please cite this article in press as: Gilbert SH, et al., Regional localisation of left ventricular sheet structure: integration with current models of cardiac fibre, sheet and band structure, Eur J Cardio-thorac Surg (2007), doi:10.1016/j.ejcts.2007.03.032

[52] Sanchez-Quintana D, Anderson RH, Ho SY. Ventricular myoarchitecture in tetralogy of Fallot. Heart 1996;76:280–6.
[53] Hort W. Untersuchungen über die Muskelfaserdehnung und das gefüllter des Myokards in der rechten Herzkammerwand des Meerschweinchens. Virchows Archiv 1957;329:694.
[54] Hort W. Makroskopische und mikrometrische Untersuchungen am Myokard verschieden stark gefüllter linker Kammern. Virchows Archiv 1960;333:523.
[55] Hort W. Mikrometrische Untersuchungen an verschieden weiten Meerschweinchenherzen. Verhandl Deut Ges Krieslaufforsch 1957;23:343–6.
[56] LeGrice IJ, Smaill BH, Chai LZ, Edgar SG, Gavin JB, Hunter PJ. Laminar structure of the heart: ventricular myocyte arrangement and connective tissue architecture in the dog. Am J Physiol 1995;269:H571–82.
[57] LeGrice IJ, Hunter PJ, Smaill BH. Laminar structure of the heart: a mathematical model. Am J Physiol 1997;272:H2466–7.
[58] Dokos S, Smaill BH, Young AA, LeGrice IJ. Shear properties of passive ventricular myocardium. Am J Physiol Heart Circ Physiol 2002; 283:H2650–9.
[59] Boineau JP. Left ventricular muscle band (VMB): thoughts on its physiologic and clinical implications. Eur J Cardiothorac Surg 2006;29:S56–60.
[60] Torrent-Guasp F, Buckberg GD, Clemente C, Cox JL, Coghlan HC, Gharib M. The structure and function of the helical heart and its buttress wrapping I. The normal macroscopic structure of the heart. Semin Thorac Cardiovasc Surg 2001;13:301–19.
[61] Robb JS, Robb RC. The normal heart – anatomy and physiology of the structural units. Am Heart J 1942;23:455–67.
[62] Torrent-Guasp F, Kocica MJ, Corno A, Komeda M, Cox J, Flotats A, Ballester-Rodes M, Carreras-Costa F. Systolic ventricular filling. Eur J Cardiothorac Surg 2004;25:376–86.
[63] Castella M, Buckberg GD, Saleh S, Gharib M. Structure function interface with sequential shortening of basal and apical components of the myocardial band. Eur J Cardiothorac Surg 2005;27:980–7.
[64] Buckberg GD. Imaging, models, and reality: a basis for anatomic-physiologic planning. Eur J Cardiothorac Surg 2005;129:243.
[65] Lunkenheimer PP, Redmann K, Kling N, Jiang X, Rothaus K, Cryer CW, Wübbeling F, Niederer P, Yen Ho S, Anderson RH. Three-dimensional architecture of the left ventricular myocardium. Anat Rec Part A 2006;288A:565–78.
[66] Lunkenheimer PP, Redmann K, Westermann P, Rothaus K, Cryer CW, Niederer P, Anderson RH. The myocardium and its fibrous matrix working in concert as a spatially netted mesh: a critical review of the purported tertiary structure of the ventricular mass. Eur J Cardiothorac Surg 2006;29:S41–9.
[67] Streeter Jr DD, Spotnitz HM, Patel DP, Ross Jr J, Sonnenblick EH. Fiber orientation in the canine left ventricle during diastole and systole. Circ Res 1969;24:339–47.
[68] Streeter DDJ, Torrent-Guasp F. Geodesic paths in the left ventricle of the mammalian heart. Circulation 1973;48:14.
[69] Nielsen PM, Le Grice IJ, Smaill BH, Hunter PJ. Mathematical model of geometry and fibrous structure of the heart. Am J Physiol 1991; 260:H1365–78.
[70] Edelman RR, Gaa J, Wedeen VJ, Loh E, Hare JM, Prasad P, Li W. In vivo measurement of water diffusion in the human heart. Magn Reson Med 1994;32:423–8.
[71] Garrido L, Wedeen VJ, Kwong KK, Spencer UM, Kantor HL. Anisotropy of water diffusion in the myocardium of the rat. Circ Res 1994;74:789–93.
[72] Jouk PS, Usson Y, Michalowicz G, Parazza F. Mapping of the orientation of myocardial cells by means of polarized light and confocal scanning laser microscopy. Microsc Res Tech 1995;30:480.
[73] Reese TG, Weisskoff RM, Smith RN, Rosen BR, Dinsmore RE, Wedeen VJ. Imaging myocardial fiber architecture in vivo with magnetic resonance. Magn Reson Med 1995;34:786–91.
[74] Vetter FJ, McCulloch AD. Three-dimensional analysis of regional cardiac function: a model of rabbit ventricular anatomy. Prog Biophys Mol Biol 1998;69:157–83.
[75] Tseng WY, Reese TG, Weisskoff RM, Wedeen VJ. Cardiac diffusion tensor MRI in vivo without strain correction. Magn Reson Med 1999;42:393–403.
[76] Holmes AA, Scollan DF, Winslow RL. Direct histological validation of diffusion tensor MRI in formaldehyde-fixed myocardium. Magn Reson Med 2000;44:157–61.
[77] Tseng WY, Reese TG, Weisskoff RM, Brady TJ, Wedeen VJ. Myocardial fiber shortening in humans: initial results of MR imaging. Radiology 2000;216:128–39.
[78] Dou J, Reese TG, Tseng WY, Wedeen VJ. Cardiac diffusion MRI without motion effects. Magn Reson Med 2002;48:105–14.
[79] Dou J, Tseng WY, Reese TG, Wedeen VJ. Combined diffusion and strain MRI reveals structure and function of human myocardial laminar sheets in vivo. Magn Reson Med 2003;50:107–13.
[80] Lunkenheimer P. The helix and the heart. Eur J Cardiothorac Surg 2003;126:920.
[81] Jiang Y, Pandya K, Smithies O, Hsu EW. Three-dimensional diffusion tensor microscopy of fixed mouse hearts. Magn Reson Med 2004;52:453–60.
[82] Buckberg GD. Stonehenge and the heart: similar construction. Eur J Cardiothorac Surg 2006;29:S286–90.
[83] Helm PA, Tseng HJ, Younes L, McVeigh ER, Winslow RL. Ex vivo 3D diffusion tensor imaging and quantification of cardiac laminar structure. Magn Reson Med 2005;54:850–9.
[84] Lunkenheimer PP, Redmann K, Anderson RH. The architecture of the ventricular mass and its functional implications for organ-preserving surgery. Eur J Cardiothorac Surg 2005;27:183.
[85] Tseng WY, Dou J, Reese TG, Wedeen VJ. Imaging myocardial fiber disarray and intramural strain hypokinesis in hypertrophic cardiomyopathy with MRI. J Magn Reson Imaging 2006;23:1–8.
[86] Costa KD, May-Newman K, Farr D, O'Dell WG, McCulloch AD, Omens JH. Three-dimensional residual strain in midanterior canine left ventricle. Am J Physiol 1997;273:H1968–76.
[87] Trew ML, Caldwell BJ, Sands GB, Hooks DA, Tai DC, Austin TM, Legrice IJ, Pullan AJ, Smaill BH. Cardiac electrophysiology and tissue structure: bridging the scale gap with a joint measurement and modelling paradigm. Exp Physiol 2006;91:355–70.
[88] Sengupta PP, Korinek J, Belohlavek M, Narula J, Vannan MA, Jahangir A, Khandheria BK. Left ventricular structure and function: basic science for cardiac imaging. J Am Coll Cardiol 2006;48:1988–2001 [Epub 2006 Oct. 1931].
[89] Antzelevitch C, Sicouri S, Litovsky SH, Lukas A, Krishnan SC, Di Diego JM, Gintant GA, Liu DW. Heterogeneity within the ventricular wall. Electrophysiology and pharmacology of epicardial, endocardial, and M cells. Circ Res 1991;69:1427–49.
[90] Trut LN. Early canid domestication: the fox-farm experiment. Am Sci 1999;87:160–9.
[91] Rijcken J, Bovendeerd PH, Schoofs AJ, van Campen DH, Arts T. Optimization of cardiac fiber orientation for homogeneous fiber strain during ejection. Ann Biomed Eng 1999;27:289–97.
[92] Van Der Bel-Kahn J. Muscle fiber disarray in common heart diseases. Am J Cardiol 1977;40:355.
[93] Rossi MA, Abreu MA, Santoro LB. Connective tissue skeleton of the human heart: a demonstration by cell-maceration scanning electron microscope method. Circulation 1998;97:934–5.
[94] Mall FP. On the muscular architecture and growth of the ventricles in the human heart. Am J Anat 1911;2:417.
[95] Torrent-Guasp F, Kocica MJ, Corno AF, Komeda M, Carreras-Costa F, Flotats A, Cosin-Aguillar J, Wen H. Towards new understanding of the heart structure and function. Eur J Cardiothorac Surg 2005; 27:191–201.

Please cite this article in press as: Gilbert SH, et al., Regional localisation of left ventricular sheet structure: integration with current models of cardiac fibre, sheet and band structure, Eur J Cardio-thorac Surg (2007), doi:10.1016/j.ejcts.2007.03.032